

**SUBSTITUTION EFFECTS ON THE 1,3-DIOXOLAN-2-YLIUM SYSTEM**

**THE STRUCTURAL EFFECTS OF SUBSTITUTION**

**ON**

**THE 1,3-DIOXOLAN-2-YLIUM SYSTEM**

**By**

**RICHARD MICHAEL ORGIAS, B.Sc.**

**A Thesis**

**Submitted to the School of Graduate Studies**

**in partial Fulfilment of the Requirements**

**for the Degree**

**Master of Science**

**McMaster University**

**(February 1989)**

MASTER OF SCIENCE (1989)

McMASTER UNIVERSITY

(Chemistry)

Hamilton, Ontario

TITLE:           The Structural Effects of Substitution on the  
                  1,3-Dioxolan -2-Ylium System

AUTHOR:          Richard Michael Orgias, B.Sc. (McMaster University)

SUPERVISOR:     Professor R.F. Childs

NUMBER OF PAGES: x, 96

## ABSTRACT

This thesis deals with O-substituted carbenium ions. In particular, the relationship between the pattern of substitution and the nature of the charge distribution in the ion are probed by looking at the effects of systematic substituent change on bond distances.

The model system employed in this investigation is the 1,3-dioxolan-2-ylum ion. A series of five ions were investigated by the preparation of single crystals which were studied using x-ray crystallography.

The carbon oxygen bond distances around the five-membered dioxolanylium ring were found to be sensitive to changes in methyl substitution at position 4 of the ring. As methyl substitution at this position was increased systematically, an increase in the C4-O3 carbon oxygen bond distance was observed.

Changes in the substituent at position 2 of the dioxolanylium ring also had an effect on carbon oxygen bond distances but of a lesser magnitude than those brought about by methyl substitutions at position 4. The importance of these changes in structure are discussed in terms of the charge distribution in the cations.

**TO MOM AND DAD**

## ACKNOWLEDGEMENTS

I would like to use this opportunity to express my gratitude to my research director, Professor R.F. Childs who has provided me with much guidance and encouragement and who has been very patient and helpful during the writing of this thesis.

I would also like to express my sincerest thanks to Dr. M. Mahendran who has provided me with both good counsel and moral support during the course of my research and the writing of this work.

Finally, I would like to acknowledge some of the others who have made the completion of this thesis possible: my Parents, Mr Romolo Faggiani, Gary, Steve, Marianne, Dan, Liz, and Doris.

## TABLE OF CONTENTS

	PAGE
DESCRIPTIVE NOTE	ii
ABSTRACT	iii
ACKNOWLEDGEMENTS	iv
LIST OF TABLES	viii
LIST OF FIGURES	x
CHAPTER 1 INTRODUCTION	
1.1 Carbenium Ions: General Background	1
1.2 Importance of Carbenium Ion Structure	2
1.3 The Study of Carbenium Ions	3
1.4 X-ray Crystallography as a Structural Probe	4
1.5 Oxygen Containing Carbenium Ions	5
1.6 Urenium Ions	7
1.7 Protonated Carboxylic Acids	10
1.8 Protonated Benzophenones	11
1.9 Systems containing Alkylated Carbonyl Groups	15
1.10 Objectives of the Present Study	18
CHAPTER 2 RESULTS AND DISCUSSION	
2.1 Preparation of Dioxolanylium Ions and Their Precursors	21
2.1.1 Ester Precursors	21
2.1.2 Dioxolanylium Ions	23

2.2	X-ray Structure Determinations of the cations <u>14b</u> - <u>18b</u>	24
2.2.1	Crystal Data for <u>14b</u>	24
2.2.2	Crystal Data for <u>15b</u>	24
2.2.3	Crystal Data for <u>16b</u>	24
2.2.4	Crystal Data for <u>17b</u>	31
2.2.5	Crystal Data for <u>18b</u>	24
2.3	Structural Features of the 1,3-Dioxolan-2-ylum Cations <u>14b</u> - <u>18b</u>	37
2.3.1	2-phenyl-1,3-dioxolan-2-ylum trifluoromethane sulfonate <u>14b</u>	38
2.3.2	2-(4-methoxyphenyl)-1,3-dioxolan-2-ylum hexafluoroantimonate <u>15b</u>	39
2.3.3	2-(2,4-pentadienyl)-1,3-dioxolan-2-ylum hexafluoroantimonat <u>16b</u>	40
2.3.4	2-(4-methoxyphenyl)-4-methyl-1,3-dioxolan-2-ylum hexafluoroantimonate <u>17b</u>	42
2.3.5	2-(4-methoxyphenyl)-4,4-dimethyl-1,3-dioxolan-2-ylum hexafluoroantimonate <u>18b</u>	43
CHAPTER 3 INTERPRETIVE DISCUSSION		
3.1	Comparative Analysis of 1,3-Dioxolan-2-ylum Cations <u>14b</u> - <u>18b</u>	46
3.1.1	Structural Features of Substituents at Position 2	46
3.1.2	The Effect of Substitution on the Dioxolanylium System	50
3.2	Concluding Remarks	57



## CHAPTER 4 EXPERIMENTAL METHODS

4.1	Instrumental Techniques	60
4.2	Purification of Solvents	60
4.3	Syntheses	61
4.4	Crystal Structure Determinations	68
APPENDIX A	TABLES OF ATOMIC POSITIONS AND TEMPERATURE FACTORS	86
REFERENCES		96

## LIST OF TABLES

		PAGE
Table 2-1	1,3-Dioxolan-2-Ylium Ions Studied	22
Table 2-2	Interatomic Distances and Angles for <u>14b</u>	25
Table 2-3	Interatomic Distances and Angles for <u>15b</u>	27
Table 2-4	Interatomic Distances and Angles for <u>16b</u>	29
Table 2-5	Interatomic Distances and Angles for <u>17b</u>	32
Table 2-6	Interatomic Distances and Angles for <u>18b</u>	35
Table 3-1	Comparison of Bond Distances in <u>16b</u> to literature values	49
Table 3-2	1,3-Dioxolan-2-Ylium five-membered ring bond distances	51
Table 4-1	<sup>1</sup> H NMR Chemical Shift Data for Esters <u>14a</u> - <u>18a</u> and Salts <u>14b</u> - <u>18b</u>	67
Table 4-2	Crystal Data for <u>14b</u>	74
Table 4-3	Crystal Data for <u>15b</u>	76
Table 4-4	Crystal Data for <u>16b</u>	78
Table 4-5	Crystal Data for <u>17b</u>	80
Table 4-6	Crystal Data for <u>18b</u>	82
Table A-1	Atomic Positional Parameters and Temperature Factors for <u>14b</u>	84
Table A-2	Hydrogen Atom Positional Parameters and Temperature Factors for <u>14b</u>	84
Table A-3	Anisotropic Temperature Factors for <u>14b</u>	85
Table A-4	Atomic Positional Parameters and Temperature Factors for <u>15b</u>	86

Table A-5	Hydrogen Atom Positional Parameters and Temperature Factors for <u>15b</u>	86
Table A-6	Anisotropic Temperature Factors for <u>15b</u>	87
Table A-7	Atomic Positional Parameters and Temperature Factors for <u>16b</u>	88
Table A-8	Hydrogen Atom Positional Parameters and Temperature Factors for <u>16b</u>	88
Table A-9	Anisotropic Temperature Factors for <u>16b</u>	89
Table A-10	Atomic Positional Parameters and Temperature Factors for <u>17b</u>	90
Table A-11	Hydrogen Atom Positional Parameters and Temperature Factors for <u>17b</u>	90
Table A-12	Anisotropic Temperature Factors for <u>17b</u>	91
Table A-13	Atomic Positional Parameters and Temperature Factors for <u>18b</u>	92
Table A-14	Hydrogen Atom Positional Parameters and Temperature Factors for <u>18b</u>	92
Table A-15	Anisotropic Temperature Factors for <u>18b</u>	93

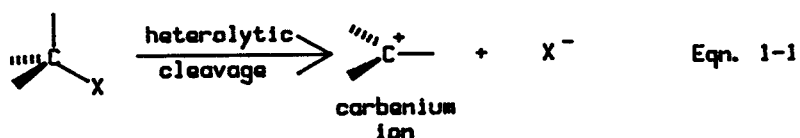
## LIST OF FIGURES

		PAGE
Figure 1-1	The t-butyl and cycloheptatrienyl cations	2
Figure 1-2	The urenium ion	7
Figure 1-3	The O-methylurenium ion	8
Figure 1-4	The N-methylurenium ion	9
Figure 1-5	The dihydroxymethyl carbenium ion	10
Figure 1-6	The protonated benzophenone carbenium ion	11
Figure 1-7	The protonated di-p-methoxybenzophenone carbenium ion	12
Figure 1-8	The protonated p-chlorobenzophenone carbenium ion	13
Figure 1-9	An Ethylated Bicyclic Lactone	15
Figure 1-10	The 2,4,4,5,5-pentamethyl-1,3-dioxolan-2-ylum cation	16
Figure 1-11	The 4,4,5,5-tetramethyl-2-phenyl-1,3-dioxolan-2-ylum ion	18
Figure 1-12	The 1,3-dioxolan-2-ylum ion	19
Figure 2-1	Snoopi Diagram of <u>14b</u>	26
Figure 2-2	Snoopi Diagram of <u>15b</u>	28
Figure 2-3	Snoopi Diagram of <u>16b</u>	30
Figure 2-4	Snoopi Diagram of <u>17b</u>	34
Figure 2-5	Snoopi Diagram of <u>18b</u>	36

CHAPTER 1  
INTRODUCTION

1.1 Carbenium Ions: General Background

The reactions of organic compounds most frequently involve the making and breaking of bonds. One of the predominant processes by which this can occur involves a heterolytic cleavage of a bond. The breaking of covalent bonds in this manner results in the separation of charge and the formation of ions. There are two basic types of heterolytic cleavage which lead to the residual carbon atom being either positively or negatively charged. The former process, illustrated in equation 1-1, gives rise to a positively charged trivalent species known as a carbenium ion.



Carbenium ions represent an ubiquitous class of reactive intermediates, which are of significant interest to the organic chemist because of the wide variety of reactions in which they participate. The existence of positively charged organic species was established nearly 90 years ago.<sup>1</sup> Some 20 years later it was suggested that they play an integral part in many of the transformations of organic chemistry.<sup>2,3</sup> Since that time, an enormous amount of effort has been dedicated to the study of these species.<sup>1,4-8</sup> These studies have shown that not only are carbenium ions widespread but that they also exhibit a great diversity of form as exemplified by the cycloheptatrienyl cation, 1, and the t-butyl cation, 2, pictured in figure 1-1.



fig 1-1

### 1.2 Importance of Carbenium Ion Structure

An understanding of structure is fundamental to achieving a full understanding of a chemical system. The structure of a molecule is one of its basic properties and has a direct impact on observable characteristics such as stability and reactivity. For example, the

determination of precise atomic coordinates will reveal the conformation assumed by a molecule in a given state . This in turn may be of use in explaining some aspect of reactivity which, up to the point of the structure solution, was not understood. In the case of reactive intermediates such as carbenium ions, structural features may help the understanding of the mechanistic nature of the reaction in which the structural motif is found.<sup>9</sup> The study of such ions is therefore a potentially useful source of information about the mechanisms of reactions in which they occur.

### 1.3 The Study of Carbenium Ions

Up to the present time, many studies have been carried out in an effort to gather information about the structure of carbenium ions. Initial studies involving the solvolyses of various chemical species in different solvent systems led early investigators to suggest that the rate of solvolysis gave some indication of the relative stability of carbenium ions.<sup>10</sup> Unusual reactivity of a system was often interpreted in terms of the structure of the ionic intermediates.

More recent research has involved the use of spectroscopic techniques to observe and characterize carbenium ions.<sup>11</sup> The development of methodologies for generating stable solutions of cations and increasing their longevity through the use of ionizing, non-nucleophilic solvents under low temperature conditions has allowed for the gathering of a large amount of spectroscopic data.<sup>12</sup> This information has proved invaluable as

a basis for achieving an understanding of the fundamental nature of these species. The most widely used spectroscopic technique in the study of cations has been NMR. Many workers have recorded the  $^1\text{H}$  and  $^{13}\text{C}$  NMR solution spectra of a large number of cations and on the basis of these have drawn conclusions regarding the charge distribution, structure, and stability of these systems.<sup>4</sup>

Other methods which have been used to probe the structure of carbenium ions include theoretical calculations, uv and microwave spectroscopy, and electron diffraction techniques.<sup>1</sup>

Although a large amount of research has been done in the area of carbenium ion structure analysis, a vanishingly small part of this work has been performed on samples in the solid state. This omission is understandable because by and large, most chemistry done is solution chemistry. However, this does not preclude the fact that there is a lot to be learned from the analysis of data obtained from solid samples. At present the most useful method for studying solid samples is x-ray crystallography.

#### 1.4 X-ray Crystallography as a Structural Probe

The compelling advantage which x-ray crystallography has over other analytical methods such as spectroscopy and theoretical calculations is its provision of direct information. Crystallography allows for the precise determination of atomic coordinates and this gives unequivocal information about structure. This is in marked contrast to other methods



which, while easier to perform, provide structural information through the subjective process of interpretive analysis.

The use of x-ray crystallography as a tool for studying carbenium ion structure is not a new concept. However, the number of good structure determinations of carbenium ions is small, due largely to the inherent reactivity of the species which make them difficult to isolate and crystallize.

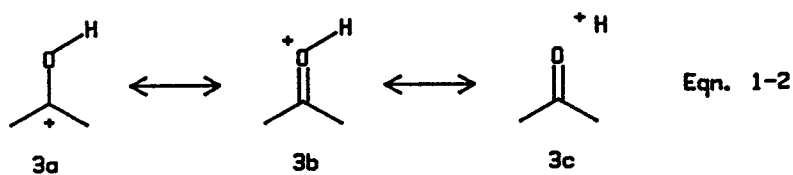
A particularly important feature of x-ray data is its presentation of chemical systems in low energy states, a situation which arises because crystallization is an energetically favourable process (i.e. energy is released during crystallization). The direct implication of this is that the conformations and other structural features observed in a given structure generally correspond to preferred orientations.

Another advantage of x-ray crystallography is its growing preeminence as a method for the routine, reliable and precise determination of atomic coordinates and its increasingly wide acceptance as a means for enhancing the understanding of chemical phenomena through a study of molecular structures.<sup>13-17</sup>

### 1.5 Oxygen Containing Carbenium Ions

An important class of carbenium ions are those in which an oxygen is attached to the trivalent carbon atom. In these systems, the charge on the C<sup>+</sup> atom can be stabilized by the lone pair on oxygen as depicted by the canonical forms shown in equation 1-2. The structure

containing the trivalent oxygen atom is known as an oxonium ion.



Oxonium ions have been studied extensively by many researchers. Two comprehensive reviews on oxonium ions, which deal with many aspects of their chemistry including nomenclature, methods of preparation, and reactivity patterns, have been published by Pittman et al<sup>18</sup> and Perst.<sup>19</sup>

Oxygen containing carbenium ions arise from the protonation or alkylation of carbonyl groups. As such, they are of interest because they are intermediates in a number of important and very useful chemical transformations of carbonyl compounds. Reactions in this category include the general acid catalyzed nucleophilic additions to the C=O bonds of ketones and aldehydes (acetal, ketal, and oxime formation for example) and acid-mediated transformations of carboxylic acid derivatives such as ester hydrolysis, amide hydrolysis, transesterification and O-alkylation.

The structure and charge distribution of carbenium ions in which the positive charge is delocalized between the carbon and oxygen of what prior to cation formation was a formal C-O double bond is a subject which

has attracted some attention but which is still not fully understood. Any attempt to enhance our understanding of the protonated carbonyl functionality must begin with an examination of its structure, conformation, and charge distribution, aspects which are important yet largely unknown.

In order to establish a frame of reference and to lay the groundwork for the later discussion, a survey of the crystal structures of some representative oxygen substituted carbenium ions is presented in the following pages.

### 1.6 Urenium Ions

The protonation or alkylation of urea and its N-alkylated derivatives gives rise to a class of ions known generically as urenium ions.

The structure of the urenium ion 4, shown in figure 1-2, has been determined in the presence of two different counter ions,  $\text{PO}_4^{-20}$  and  $\text{NO}_3^{-.21}$

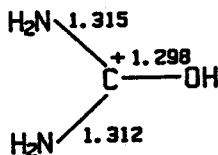


fig. 1-2 (4)

An examination of the bond lengths in the carbenium ion of the urenum nitrate structure reveals a C=O bond length of 1.298Å and C-N bond lengths of 1.315Å and 1.312Å. A comparison of these values with those of urea indicate a lengthening of the C=O double bond accompanied by the concomitant shortening of the two C-N bonds.<sup>22,23</sup> This is consistent with a structure in which the positive charge has been delocalized over the entire framework of the molecule thereby reducing the energy of the system through heteroatom stabilization.

A structural determination of O-methylurenum hydrochloride yielded bond length information for the O-methylurenum ion, 5, presented in figure 1-3.<sup>24</sup>

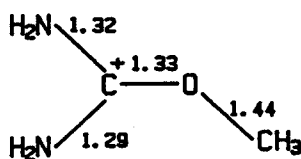


fig. 1-3 (5)

This carbenium ion shows a trend in bond lengths similar to that observed for 4. The C=O distance observed in this instance is 1.33Å and the C-N distances are 1.29Å and 1.32Å. Again the lengthening of the C=O bond and the shortening of the C-N bonds can be attributed to heteroatom stabilization resulting in the distribution of charge over the molecular

framework. The O-methylated urea displays a longer C=O bond distance than its protonated counterpart, possibly the result of the superior hydrogen bonding abilities of the proton over the methyl group. The CH<sub>3</sub>-O distance of 1.44Å is consistent with the average bond length of 1.426Å observed in dialkyl ethers.<sup>25</sup>

The structure depicted in figure 1-4 is that of the N-methylurenum ion, 6.<sup>26</sup> This ion, isolated in the form of its nitrate salt, exhibits a C=O bond length of 1.28Å and C<sup>+</sup>-N distances of 1.29Å and 1.30Å. The C=O and C<sup>+</sup>-N bond lengths in this compound display the same trends observed for the urenum ions, 4 and 5, considered above. The planarity of all three ions is indicative of the partial double bond character of the C=O and C-N bonds.

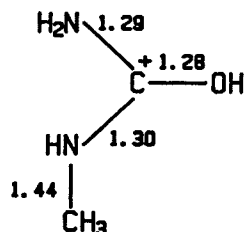


fig. 1-4 (6)

### 1.7 Protonated Carboxylic Acids

Structural data on two 1:1 adducts of acetic acid with inorganic acids have been obtained. One structure determination is of protonated acetic acid, 7, isolated as a fluorosulfate salt (figure 1-5) and the other of the hydrogen sulfate salt.<sup>27,28</sup>

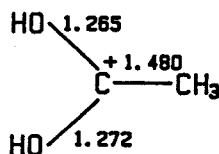


fig. 1-5 (7)

The C-O bond lengths of 1.265Å and 1.272Å are the same within the limits of experimental error and clearly represent values intermediate to those of the C=O double and single bonds. The carbon-oxygen distances observed in carboxylic acids are 1.214(19)Å for the C=O bond and 1.308(19)Å for the C-OH bond.<sup>25</sup>

The non-hydrogen atoms are coplanar in this structure and the C<sup>+</sup>-C distance is 1.480Å, a value which points to the increased bond order of the linkage [cf. 1.465(18)Å for C(sp<sup>2</sup>)-C(sp<sup>2</sup>)<sup>25</sup> and 1.507(15)Å for C(sp<sup>3</sup>)-C(sp<sup>2</sup>)<sup>25</sup>]. This shortening of the C-C bond has been attributed to the hyperconjugative interaction between the methyl group and the electron deficient carbon centre.<sup>28</sup>

### 1.8 Protonated Benzophenones

An x-ray crystallographic study performed on a series of protonated benzophenones isolated as crystalline ionic salts provides additional structural information on oxonium ion species.<sup>29</sup>

The protonated benzophenone cation, 8, shown in figure 1-6 was isolated as its hexafluoroantimonate salt and its crystal structure determined.

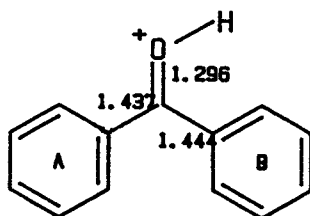


fig 1-6 (B)

The C=O distance observed in this molecule is 1.296Å and the C<sup>+</sup>-Ar bond distances are 1.437Å and 1.449Å. As was observed in the urenum ion systems, the presence of a heteroatom or some other functionality (R) capable of delocalizing charge adjacent to the electron deficient carbonyl carbon coincides with the lengthening of the C=O bond and the contracting of the C<sup>+</sup>-R bonds relative to the neutral system.<sup>30</sup>

Another observed structural feature of 8 is the twist of the phenyl rings from the C-C(O)-C plane. The observed values of this deformation for 9 are 28° for the A ring and 31.8° for the B ring.

A counterpart to 8 is the protonated di-*p*-methoxybenzophenone, 9, prepared in the presence of the fluorosulfate anion and depicted in figure 1-7.

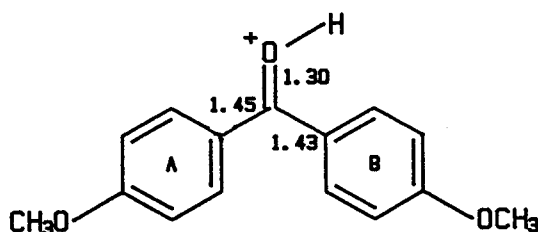


fig. 1-7 (9)

The electron donating *p*-methoxy substituents are built in probes designed to detect the variation of bond lengths with the ability of a functional grouping to satisfy the electron demand of the charge bearing locus. In a system such as this, the para methoxy groups would be expected to stabilize the ion and one would expect to observe a longer carbonyl bond and shorter bonds between position 1 of the benzene rings and the electron deficient carbon atom. In this instance the observed C=O bond length is 1.30Å and the C<sup>+</sup>-Ar bond lengths are 1.45Å and 1.43Å. Again a lengthening of the C=O bond and the contraction of the C<sup>+</sup>-Ar bond is observed indicating the delocalization of charge within the system. The observed twist angles of the phenyl rings from the C-C(O)-C plane are 30° for ring A and 24° for ring B. These values for the twist angles are smaller than those observed for 8.



The protonated p-chlorobenzophenone cation 10, prepared as a hexafluoroantimonate salt is the third member in the series of protonated benzophenones. This carbenium ion is unusual in that it was isolated as a dimer. In this system the carbonyl oxygen of one species was bonded to the oxygen of another p-substituted chlorobenzophenone by a hydrogen bond. The O...O bond distance in this structure was 2.468Å. The structure of this carbenium ion system pictured in figure 1-8 is interesting because the introduction of a chlorine in the para position of the B rings should have a destabilizing effect on the cation as a whole.

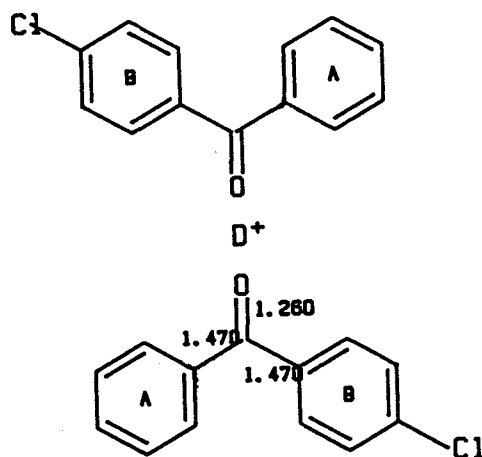


fig. 1-8 (10)

The C-O bond length in this structure is 1.260Å, the shortest of the three C-O distances encountered in the series. The two C<sup>+</sup>-Ar bond lengths at 1.470Å are the longest C<sup>+</sup>-Ar bonds observed in the three compounds.

Twist angles about the C-C(O)-C plane for the A and B rings are 17.9° and 43.3° respectively. The dramatic difference in the twist angles of the A ring and the chlorine bearing B ring is perhaps significant. Such a twisting of the B ring out of conjugation, ostensibly to alleviate its destabilizing effect on the carbenium ion is consistent with what is known regarding the effect of electron withdrawing and electron donating substituents on charge bearing centres.

If all three protonated benzophenones 8, 9, and 10, are considered together, systematic changes in some gross features of these ions become evident. It is clear that all three structures differ from neutral benzophenone which has a C=O bond length of 1.23(1)Å and C-Ar bond lengths of 1.48(1)Å and 1.50(1)Å.<sup>30</sup> This is an expected difference since the charge distribution of a neutral system differs from that of a protonated system.

A more thorough examination of the structures suggests a more subtle relationship, that of a linear correlation between the C-O distances and the C-Ar distances in the neutral and protonated species. It has been suggested that systematic changes in these two bond distances are related to the overall stability of the cation.<sup>29</sup>

### 1.9 Systems Containing Alkylated Carbonyl Groups

In all the benzophenone and urenium ion structures discussed so far, there is always a strong hydrogen bond formed between the OH proton and an atom in the counterion present in the crystal lattice. The implication of this phenomenon is that the full effect of protonation is not felt by any single cationic entity, rather the effect is diminished by the hydrogen bonding interaction.

A number of x-ray structural analyses have been performed on carbenium ions in which an alkyl substituent rather than a proton has been added to a carbonyl oxygen. It is interesting that these are found to exhibit similar C=O bond distances and other structural features characteristic of the protonated carbonyls. The advantage of using such O-alkylated systems as models for protonated carbonyls is that they allow more precise determination of the bond distances and angles around oxygen.

Examples of O-alkylated cations are provided by lactonium salts which can be prepared by the ethylation of lactones with Meerwein's reagent. The ethylated lactone 11, a diagram of which appears in figure 1-9 bears some interesting structural features.<sup>29</sup>

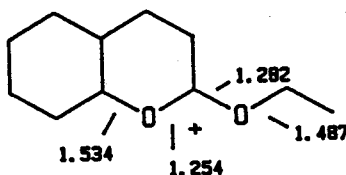


fig. 1-9 (11)

The C<sup>+</sup>-O bond lengths observed in this structure are 1.254Å and 1.282Å, both of which are longer than a C=O double bond, shorter than a C-O single bond and comparable to the lengths found in protonated carbonyls.

The internuclear distances of the C-O single bonds present in this molecule are also of interest. These bond lengths are important because they provide insight into the nature of the charge distribution in these systems. Of special note is the unusually long 1.534Å distance of the linkage between the ring oxygen and the adjacent secondary carbon. It has been suggested that this long internuclear distance is indicative of positive charge being transferred to the tertiary carbon bonded to the ring oxygen.<sup>29</sup>

Figure 1-10 shows the 2,4,4,5,5-pentamethyl-1,3-dioxolan-2-ylum cation 12, which has been isolated as a perchlorate salt.<sup>31</sup>

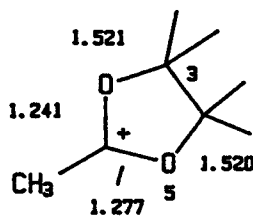


fig. 1-10 (12)

In this carbenium ion, the five-membered dioxolanylium ring is planar and the acetoxonium methyl group is coplanar with the ring.

The C<sup>+</sup>-O bond lengths are 1.241Å and 1.277Å, typical of the values observed in the other systems presented thus far. The C-O bond distances at 1.521Å (C3-O2) and 1.520Å (C4-O5) are long for C-O single bonds, the average length of such bonds in alkyl esters of benzoic acid being about 1.454(12)Å <sup>25</sup>

The two pairs of methyl groups at the 4 and 5 position of the five-membered ring adopt a sterically unfavourable eclipsed position, good evidence in support of stabilization imparted by conjugation between the oxygens and the trigonal carbon. Efficient overlap of the atomic orbitals participating in the delocalization requires the planar arrangement of the ring which in turn gives rise to the energetically unfavourable steric interaction between the methyl groups. <sup>31</sup>

A further example of this type of cation is provided in the structure of the 4,4,5,5-tetramethyl-2-phenyl-1,3-dioxolan-2ylium cation 13 shown in figure 1-11 which was prepared as its dichloroiodate salt. <sup>32</sup> This material possesses structural features which are similar to those observed in 12.

The dioxolanylium and phenyl rings are planar and the system as a whole exhibits planarity. As was observed in 12, the methyl groups of the dioxolanylium ring adopt an eclipsed conformation. The observed C<sup>+</sup>-O distance in this system is 1.29Å and the C-O distance is 1.52Å. Here as before, lengthening of the C<sup>+</sup>-O bonds as compared to the standard

C=O value is observed. The C-Ar value of 1.47Å is unexceptional and compares closely to that observed in benzoate esters [1.487(12)Å]<sup>25</sup>

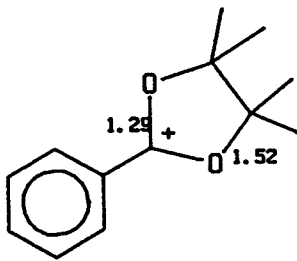


fig. 1-11 (13)

In addition to the representative carbenium ion structures presented above, there are a number of oxygen containing carbenium ions for which structural data has been published.<sup>29, 33, 34</sup> Among them are a pair of cyclopropenium ions, a pair of cyclopropylcarbiny cations and a hydroxyhomotropylium cation. These ions display similar trends in bond lengths to those ions already presented and will not be discussed further in this thesis.

#### 1.10 Objectives of the Present Study

The limited number of oxygen containing cations whose structures have been determined have been presented in the preceding part of this chapter. These cations represent a variety of different systems. While general trends such as the lengthening of a C=O bond on protonation or alkylation is evident, it is more difficult to pull out systematic trends.

The purpose of the work described in this thesis was to examine in more detail the structural effects of substitution on an oxygen containing carbenium ion. It was intended to focus attention on a single type of system and look at the effects of systematic substituent changes. The intent of the study was to systematically probe the charge distribution in a  $\text{C}^+-\text{OR}$  containing cation and on the basis of the results make an assessment of the relative importance of the various resonance contributors shown in equation 1-2.

The model system chosen for this work was the 1,3-dioxolan-2-ylum cation shown in figure 1-12. This system satisfied our requirements for an easily modified, well characterized, ( in terms of other techniques) oxygen containing carbenium ion system suitable for a study of the geometric changes associated with the introduction of positive charge at a carbon centre bonded to oxygen.

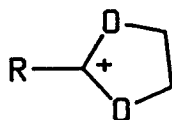
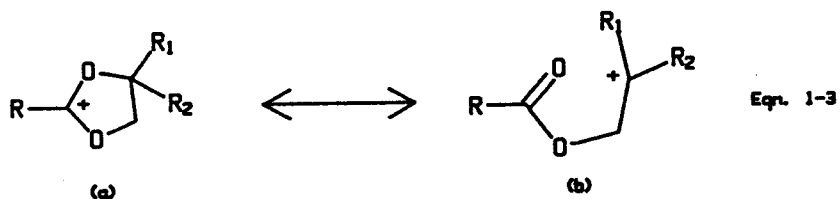


fig. 1-12

The dioxolanylium system also allowed us to examine the structural effects of two different types of asymmetric substitution . The first

approach involved changing the substituent at position 2 of the dioxolanylium ring, leaving the rest of the molecule constant. This allowed the observation of how the ability of the substituent at position 2 to delocalize charge affected the length of the C-O bonds. The second approach was meant to assess the importance of the resonance structure b of equation 1-3, in the overall description of the ground state of the cation. This was accomplished by varying the degree of methyl substitution at position 4 of the dioxolanylium ring. Both of these approaches could be used in a qualitative sense to determine where the bulk of the positive charge in the system resides.





CHAPTER 2  
RESULTS AND DISCUSSION

2.1 Preparation of Dioxolanylium Ions and Their Precursors

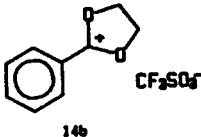
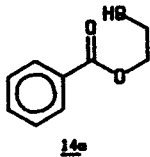
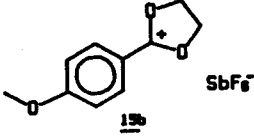
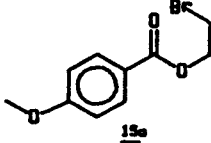
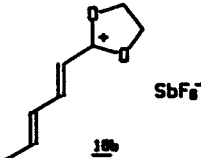
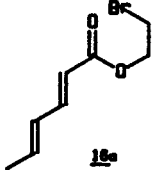
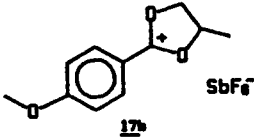
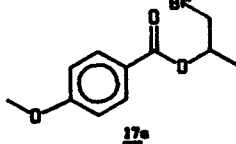
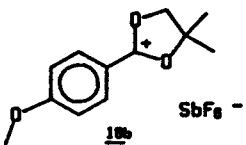
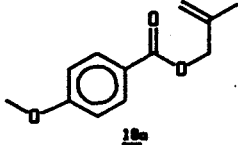
A total of five dioxolanylium cations were prepared in a form suitable for analysis using x-ray diffraction techniques. The carbenium ions studied by crystallography, 14b - 18b, and the esters, 14a - 18a from which they were made appear in table 2-1.

2.1.1 Ester precursors

The first step in our study of the five 1,3-dioxolan-2-ylium salts surveyed involved the preparation of the ester precursors (14a - 18a) of the compounds. The esters were prepared as described in the experimental section of this thesis and characterized using  $^1\text{H}$  NMR methods. The three esters which do not bear substituents in the alcohol-derived part of the molecule (14a, 15a, and 16a) share a characteristic  $^1\text{H}$  NMR signal arising from the resonances of their methylene hydrogens which resonate in the region between  $\delta 3\text{ppm}$  -  $\delta 5\text{ppm}$ . The two other esters gave NMR spectra consistent with their structure. Spectral data for 14a to 15a are presented in table 4-1.

TABLE 2-1

## 1,3-Dioxolan-2-ylum Ions Studied and their Ester Precursors

Carbenium Ion	Ester Precursor
 <u>14b</u>	 <u>14a</u>
 <u>15b</u>	 <u>15a</u>
 <u>16b</u>	 <u>16a</u>
 <u>17b</u>	 <u>17a</u>
 <u>18b</u>	 <u>18a</u>

### 2.1.2 Dioxolanylium ions

The carbenium ion salt of 14b was obtained from the ester, 14a, by the addition of trifluoromethanesulfonic anhydride.<sup>35</sup> The salts of ions 15b, 16b, and 17b were obtained from their precursor esters ( 15a, 16a, and 17a ) by the addition of silver hexafluoroantimonate.<sup>36</sup> The addition of hexafluoroantimonic acid to the ester, 18a yielded the carbenium ion salt of 18b.<sup>37</sup>

Single crystals suitable for study by x-ray crystallography were obtained by recrystallization of the salts of 14b - 18b from methylene chloride.

<sup>1</sup>H NMR spectra of the compounds 14b, 15b, 16b in deuterated methylene chloride were obtained and the results are reported in table 4-1. The <sup>1</sup>H NMR spectra for the three ions which do not bear substituents in the five-membered ring (14b, 15b, and 16b) exhibit a characteristic sharp singlet corresponding to the ring methylene protons in the region  $\delta 5.0$  ppm. Good quality <sup>1</sup>H NMR spectra of the salts 17b and 18b could not be obtained

### 2.2 X-ray Structure Determinations of the Cations 14b - 18b

The crystal structures of the salts of the ions, 14b - 18b, were determined by single crystal x-ray crystallography.

All structures were refined using the computer program SHELX.<sup>38</sup> Further details regarding the methods of crystal selection, data collection and structure solution are presented in the experimental

section (Chapter 4).

### 2.2.1 Crystal Data for 14b

The space group of 14b was found to be  $C2/c$  and the appropriate reflections were collected. The crystal structure was solved using a combination of direct and difference methods and refined to an R factor of 0.049. Interatomic distances and bond angles for 14b are given in table 2-2. A Snoopi drawing of the carbenium ion is shown in figure 2-1.

### 2.2.2 Crystal Data for 15b

The space group of 15b was determined by precession photography to be  $P2_1/c$  and a suitable data set was collected. Structure solution was effected using a Patterson synthesis combined with difference methods and the structure was refined to an R of .055. The hexafluoroantimonate anion of this structure was disordered. Listings of interatomic distances and bond angles are given in table 2-3 and a Snoopi diagram of the cation is presented in figure 2-2.

### 2.2.3 Crystal Data for 16b

Precession photographs of 16b indicated that the space group was  $P2_1/c$ . Data was collected and the structure solved and refined by Patterson and difference methods to an R of .0337. A listing of relevant interatomic distances and bond angles appear in table 2-4. Figure 2-3 shows a Snoopi diagram of the ion, 16b.

Table 2-2

Bond Distances (Å) and Angles (deg.) for 2-phenyl-1,3-dioxolan-2-ylum trifluoromethanesulfonate, 14b

## Bond Distances:

S(1)-O(1)	1.430(7)	S(1)-O(2)	1.431(2)
S(1)-O(3)	1.438(3)	S(1)-C(1)	1.811(3)
C(1)-F(1)	1.322(3)	C(1)-F(2)	1.327(3)
C(1)-F(3)	1.326(4)		
C(11)-O(11)	1.282(3)	O(11)-C(12)	1.472(3)
C(12)-C(13)	1.505(5)	C(13)-O(12)	1.480(3)
C(11)-O(12)	1.281(3)	C(11)-C(21)	1.442(3)
C(21)-C(22)	1.391(4)	C(22)-C(23)	1.377(4)
C(23)-C(24)	1.374(4)	C(24)-C(25)	1.382(4)
C(25)-C(26)	1.399(4)	C(26)-C(11)	1.399(4)

## Bond Angles:

O(1)-S(1)-O(2)	115.1(1)	O(1)-S(1)-O(3)	115.8(1)
O(1)-S(1)-C(1)	102.8(1)	O(2)-S(1)-O(3)	114.2(1)
O(2)-S(1)-C(1)	103.0(1)	O(3)-S(1)-C(1)	103.4(1)
F(1)-C(1)-F(2)	106.8(2)	F(1)-C(1)-F(3)	108.1(2)
F(1)-C(1)-S(1)	111.7(2)	F(2)-C(1)-F(3)	106.9(2)
F(2)-C(1)-S(1)	111.6(2)	F(3)-C(1)-S(1)	111.4(2)
C(11)-O(11)-C(12)	108.6(2)	O(11)-C(12)-C(13)	103.1(2)
C(12)-C(13)-O(12)	103.4(2)	C(13)-O(12)-C(11)	108.1(2)
O(12)-C(11)-O(11)	116.8(2)	O(11)-C(11)-C(21)	121.1(2)
O(12)-C(11)-C(21)	122.1(2)	C(11)-C(21)-C(22)	120.0(2)
C(11)-C(21)-C(26)	119.4(2)	C(21)-C(22)-C(23)	119.6(3)
C(22)-C(23)-C(24)	120.0(3)	C(23)-C(24)-C(25)	121.0(2)
C(24)-C(25)-C(26)	120.2(3)	C(25)-C(26)-C(21)	118.7(3)
C(26)-C(21)-C(22)	120.6(2)		

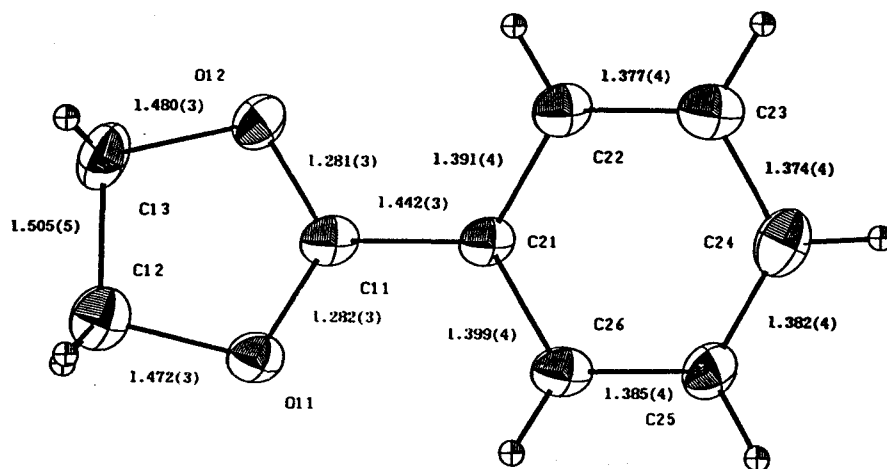


fig. 2-1. SNOOPI diagram of 14b

Table 2-3

Bond Distances (Å) and Angles (deg.) for 2-(4-methoxyphenyl)-1,3-dioxolan-2-ylum hexafluoroantimonate, 15b

## Bond Distances:

Sb(1)-F(1)	1.864(4)	Sb(1)-F(2)	1.880(5)
Sb(1)-F(3)	1.892(10)	Sb(1)-F(4)	1.838(9)
Sb(1)-F(5)	1.882(12)	Sb(1)-F(6)	1.841(11)
Sb(1)-F(11)	1.812(14)	Sb(1)-F(21)	1.865(14)
Sb(1)-F(31)	1.931(9)	Sb(1)-F(41)	1.856(10)
C(11)-O(11)	1.293(9)	O(11)-C(12)	1.474(9)
C(12)-C(13)	1.503(11)	C(13)-O(12)	1.466(9)
C(11)-O(12)	1.292(8)	C(11)-C(21)	1.414(9)
C(21)-C(22)	1.408(12)	C(22)-C(23)	1.350(10)
C(23)-C(24)	1.402(11)	C(24)-C(25)	1.405(11)
C(25)-C(26)	1.359(9)	C(26)-C(21)	1.404(12)
C(24)-O(31)	1.348(8)	O(31)-C(31)	1.444(11)

## Bond Angles:

F(1)-Sb(1)-F(2)	178.8(2)	F(1)-Sb(1)-F(3)	89.8(3)
F(1)-Sb(1)-F(4)	89.4(3)	F(1)-Sb(1)-F(5)	86.6(4)
F(1)-Sb(1)-F(6)	94.9(4)	F(2)-Sb(1)-F(3)	89.5(3)
F(2)-Sb(1)-F(4)	91.2(3)	F(2)-Sb(1)-F(5)	92.2(4)
F(2)-Sb(1)-F(6)	86.3(4)	F(3)-Sb(1)-F(4)	178.3(4)
F(3)-Sb(1)-F(5)	73.2(6)	F(3)-Sb(1)-F(6)	104.3(5)
F(4)-Sb(1)-F(5)	108.4(5)	F(4)-Sb(1)-F(6)	74.2(5)
F(5)-Sb(1)-F(6)	177.1(6)		
F(11)-Sb(1)-F(21)	178.1(6)	F(11)-Sb(1)-F(31)	70.1(5)
F(11)-Sb(1)-F(41)	107.2(5)	F(21)-Sb(1)-F(31)	111.9(5)
F(21)-Sb(1)-F(41)	70.9(5)	F(31)-Sb(1)-F(41)	176.2(5)
C(11)-O(11)-C(12)	108.7(6)	O(11)-C(12)-C(13)	103.5(6)
C(12)-C(13)-O(12)	103.2(6)	C(13)-O(12)-C(11)	109.3(6)
O(12)-C(11)-O(11)	115.6(6)	O(11)-C(11)-C(21)	
O(12)-C(11)-C(21)		C(11)-C(21)-C(22)	121.1(7)
C(11)-C(21)-C(26)	119.3(7)	C(21)-C(22)-C(23)	120.2(8)
C(22)-C(23)-C(24)	120.8(7)	C(23)-C(24)-C(25)	118.8(6)
C(24)-C(25)-C(26)	120.6(7)	C(25)-C(26)-C(21)	120.0(7)
C(26)-C(21)-C(22)	119.6(6)	C(23)-C(24)-O(31)	116.7(7)
C(25)-C(24)-O(31)	124.5(7)	C(24)-O(31)-C(31)	120.0(6)

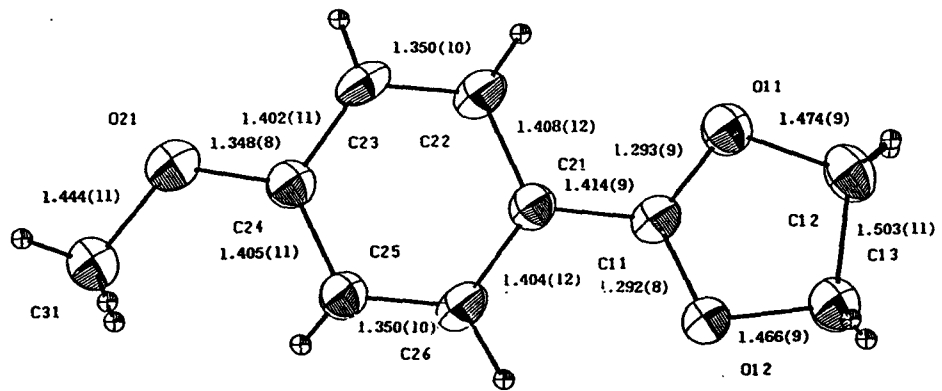


fig. 2-2 SNOOPI diagram of 15b



Table 2-4

Bond Distances (Å) and angles (deg.) for 2-(2,4-pentadienyl)-1,3-dioxolan-2-ylum hexafluoroantimonate, 16b

## Bond Distances:

Sb(1)-F(1)	1.869(3)	Sb(1)-F(2)	1.870(2)
Sb(1)-F(3)	1.868(2)	Sb(1)-F(4)	1.869(2)
Sb(1)-F(5)	1.869(2)	Sb(1)-F(6)	1.858(2)
C(11)-O(11)	1.288(5)	O(11)-C(12)	1.472(5)
C(12)-C(13)	1.515(7)	C(13)-O(12)	1.469(5)
C(11)-O(12)	1.290(5)	C(11)-C(2)	1.417(5)
C(2)-C(3)	1.349(6)	C(3)-C(4)	1.435(5)
C(4)-C(5)	1.324(6)	C(5)-C(6)	1.482(6)

## Bond Angles:

F(1)-Sb(1)-F(2)	178.0(1)	F(1)-Sb(1)-F(3)	89.0(1)
F(1)-Sb(1)-F(4)	89.2(1)	F(1)-Sb(1)-F(5)	90.8(1)
F(1)-Sb(1)-F(6)	90.6(1)	F(2)-Sb(1)-F(3)	89.3(1)
F(2)-Sb(1)-F(4)	89.6(1)	F(2)-Sb(1)-F(5)	90.8(1)
F(2)-Sb(1)-F(6)	90.7(1)	F(3)-Sb(1)-F(4)	90.1(1)
F(3)-Sb(1)-F(5)	178.6(1)	F(3)-Sb(1)-F(6)	91.1(1)
F(4)-Sb(1)-F(5)	88.5(1)	F(4)-Sb(1)-F(6)	178.8(1)
F(5)-Sb(1)-F(6)	90.3(1)		
C(11)-O(11)-C(12)	108.7(3)	O(11)-C(12)-C(13)	103.2(3)
C(12)-C(13)-O(12)	103.0(3)	C(13)-O(12)-C(11)	109.0(3)
O(12)-C(11)-O(11)	115.9(3)	O(11)-C(11)-C(2)	121.5(4)
O(12)-C(11)-C(2)	122.6(4)	C(11)-C(2)-C(3)	120.4(4)
C(2)-C(3)-C(4)	125.3(4)	C(3)-C(4)-C(5)	121.4(4)
C(4)-C(5)-C(6)	127.3(4)		

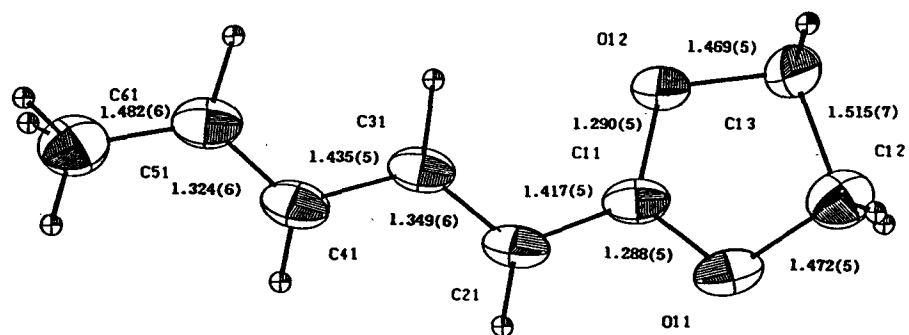


fig. 2-3 SNOOPI diagram of 16b

#### 2.2.4 Crystal Data for 17b

The space group of 17b was established as being  $Pna2_1$  by precession photography and an appropriate data set was collected. A solution to the structure was arrived at through the use of a Patterson synthesis in conjunction with difference methods. The final value of R for this structure was .0682. The hexafluoroantimonate anion was disordered and the structure was solved with the fluorines assigned partial occupancy. Interatomic distances and bond angles are given in table 2-5 and a Snoopi diagram of the ion is presented in figure 2-4.

#### 2.2.5 Crystal Data for 18b

Precession photography was used to determine the space group of 18b to be  $Pna2_1$  and a set of reflection data was collected. The structure was solved utilizing a Patterson synthesis followed by a refinement by difference methods to an R of .0796. The quality of this structure was poor. A disorder problem existed in the hexafluoroantimonate anion and the structure solution involved assigning partial occupancy to the fluorines of the anion. A listing of bond lengths and angles is presented in table 2-6. A Snoopi diagram of the cation appears in figure 2-5.

Table 2-5

Bond Distances (Å) and Angles (deg.) for 2-(4-methoxyphenyl)-4-methyl-1,3-dioxolan-2-ylum hexafluoroantimonate, 17b

## Bond Distances:

Sb(1)-F(1)	1.798(16)	Sb(1)-F(2)	1.817(24)
Sb(1)-F(3)	1.876(12)	Sb(1)-F(4)	1.830(14)
Sb(1)-F(5)	1.933(16)	Sb(1)-F(6)	1.932(18)
Sb(1)-F(11)	1.833(25)	Sb(1)-F(21)	1.909(21)
Sb(1)-F(31)	1.815(25)	Sb(1)-F(41)	1.940(18)
Sb(1)-F(51)	1.864(26)	Sb(1)-F(61)	1.947(23)
C(11)-O(11)	1.291(10)	O(11)-C(12)	1.476(13)
C(12)-C(13)	1.567(14)	C(13)-C(131)	1.319(36)
C(13)-O(12)	1.503(12)	C(11)-O(12)	1.274(11)
C(11)-C(21)	1.441(13)	C(21)-C(22)	1.410(14)
C(22)-C(23)	1.391(14)	C(23)-C(24)	1.381(15)
C(24)-C(25)	1.392(15)	C(25)-C(26)	1.371(14)
C(26)-C(21)	1.398(12)	C(24)-O(31)	1.348(13)
O(31)-C(31)	1.480(15)		

## Bond Angles:

F(1)-Sb(1)-F(2)	171.4(9)	F(1)-Sb(1)-F(3)	95.9(7)
F(1)-Sb(1)-F(4)	81.4(7)	F(1)-Sb(1)-F(5)	97.2(8)
F(1)-Sb(1)-F(6)	84.6(9)	F(2)-Sb(1)-F(3)	89.8(8)
F(2)-Sb(1)-F(4)	93.2(7)	F(2)-Sb(1)-F(5)	89.4(7)
F(2)-Sb(1)-F(6)	89.6(10)	F(3)-Sb(1)-F(4)	176.3(7)
F(3)-Sb(1)-F(5)	88.3(7)	F(3)-Sb(1)-F(6)	84.0(7)
F(4)-Sb(1)-F(5)	89.5(7)	F(4)-Sb(1)-F(6)	98.2(7)
F(5)-Sb(1)-F(6)	172.3(7)		
F(11)-Sb(1)-F(21)	88.2(11)	F(11)-Sb(1)-F(31)	90.9(12)
F(11)-Sb(1)-F(41)	102.3(10)	F(11)-Sb(1)-F(51)	121.7(11)
F(11)-Sb(1)-F(61)	86.2(10)	F(21)-Sb(1)-F(31)	177.7(10)
F(21)-Sb(1)-F(41)	145.3(9)	F(21)-Sb(1)-F(51)	57.7(10)
F(21)-Sb(1)-F(61)	86.1(10)	F(31)-Sb(1)-F(41)	37.0(10)
F(31)-Sb(1)-F(51)	124.5(11)	F(31)-Sb(1)-F(61)	91.7(10)
F(41)-Sb(1)-F(51)	89.3(10)	F(41)-Sb(1)-F(61)	127.2(9)
F(51)-Sb(1)-F(61)	130.1(11)		

C(11)-O(11)-C(12)	108.7(8)	O(11)-C(12)-C(13)	103.1(8)
C(12)-C(13)-O(12)	100.6(8)	C(12)-C(13)-C(131)	119(2)
O(12)-C(13)-C(131)	112(2)	C(13)-O(12)-C(11)	109.8(7)
O(12)-C(11)-O(11)	117.0(8)	O(11)-C(11)-C(21)	122.2(8)
O(12)-C(11)-C(21)	120.4(9)	C(11)-C(21)-C(22)	118.3(9)
C(11)-C(21)-C(26)	119.2(9)	C(21)-C(22)-C(23)	119(1)
C(22)-C(23)-C(24)	119.9(9)	C(23)-C(24)-C(25)	120.1(9)
C(24)-C(25)-C(26)	120.2(9)	C(25)-C(26)-C(21)	119.6(9)
C(26)-C(21)-C(22)	118.5(9)	C(23)-C(24)-O(31)	124.0(9)
C(25)-C(24)-O(31)	115.5(9)	C(24)-O(31)-C(31)	114.4(9)

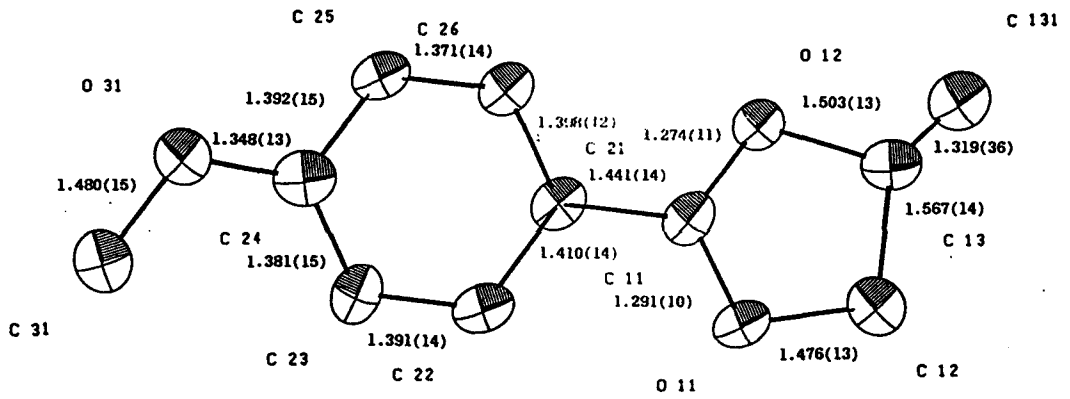


fig. 2-4 SNOOPI diagram of 17b

Table 2-6

Bond Distances (Å) and Angles (deg.) for 2-(4-methoxyphenyl)-4,4-dimethyl-1,3-dioxolan-2-ylum hexafluoroantimonate, 18b

## Bond Distances:

Sb(1)-F(1)	1.888(17)	Sb(1)-F(2)	1.876(9)
Sb(1)-F(3)	1.901(20)	Sb(1)-F(4)	1.889(23)
Sb(1)-F(5)	1.862(17)	Sb(1)-F(6)	1.884(8)
C(11)-O(11)	1.286(15)	O(11)-C(12)	1.486(17)
C(12)-C(13)	1.574(19)	C(13)-C(131)	1.590(33)
C(13)-C(132)	1.432(27)	C(13)-O(12)	1.546(15)
C(11)-O(12)	1.306(16)	C(11)-C(21)	1.409(19)
C(21)-C(22)	1.399(20)	C(22)-C(23)	1.413(19)
C(23)-C(24)	1.373(20)	C(24)-C(25)	1.462(23)
C(25)-C(26)	1.397(22)	C(26)-C(21)	1.407(20)
C(24)-O(31)	1.435(19)	O(31)-C(31)	1.445(20)

## Bond Angles:

F(1)-Sb(1)-F(2)	90.4(6)	F(1)-Sb(1)-F(3)	173.7(7)
F(1)-Sb(1)-F(4)	93.1(9)	F(1)-Sb(1)-F(5)	89.2(7)
F(1)-Sb(1)-F(6)	83.2(6)	F(2)-Sb(1)-F(3)	95.6(7)
F(2)-Sb(1)-F(4)	84.9(7)	F(2)-Sb(1)-F(5)	89.3(7)
F(2)-Sb(1)-F(6)	170.8(8)	F(3)-Sb(1)-F(4)	89.3(9)
F(3)-Sb(1)-F(5)	89.0(8)	F(3)-Sb(1)-F(6)	91.0(6)
F(4)-Sb(1)-F(5)	173.7(7)	F(4)-Sb(1)-F(6)	88.8(7)
F(5)-Sb(1)-F(6)	97.3(6)		
C(11)-O(11)-C(12)	111(1)	O(11)-C(12)-C(13)	103(1)
C(12)-C(13)-O(12)	100(1)	C(12)-C(13)-C(131)	111(2)
C(12)-C(13)-C(132)	117(2)	O(12)-C(13)-C(131)	88(1)
O(12)-C(13)-C(132)	123(1)	C(13)-O(12)-C(11)	109(1)
O(12)-C(11)-O(11)	114(1)	O(11)-C(11)-C(21)	125(1)
O(12)-C(11)-C(21)	120(1)	C(11)-C(21)-C(22)	121(1)
C(11)-C(21)-C(26)	119(1)	C(21)-C(22)-C(23)	119(1)
C(22)-C(23)-C(24)	120(1)	C(23)-C(24)-C(25)	118(1)
C(24)-C(25)-C(26)	115(1)	C(25)-C(26)-C(21)	119(1)
C(26)-C(21)-C(22)	119(1)	C(23)-C(24)-O(31)	111(1)
C(25)-C(24)-O(31)	111(1)	C(24)-O(31)-C(31)	116(1)

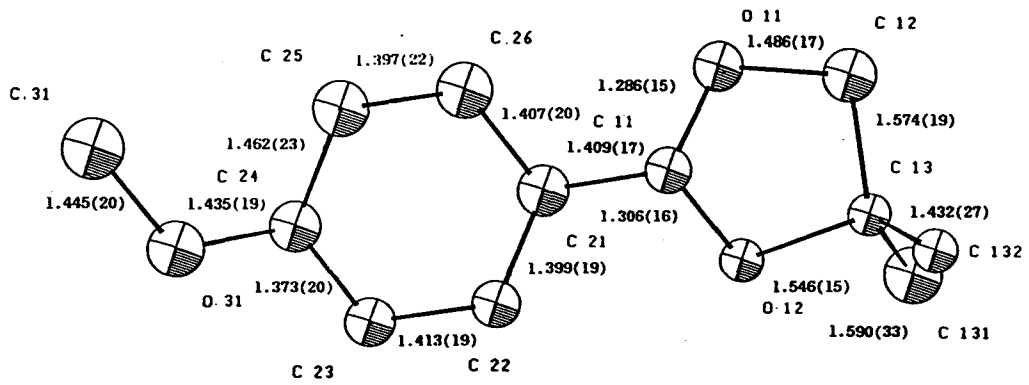
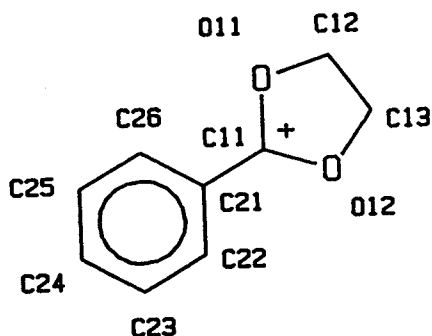


fig. 2-5 SNOOPI diagram of 18b



### 2.3 Structural Features of the 1,3-Dioxolan-2-Ylium Cations 14b - 18b

Much of the ensuing discussion is focussed on bond distances and more importantly on the differences or similarities observed in similar bonds in different compounds. In order to facilitate this comparison, the same system of numbering has been used in the five ions studied. A guide to the numbering system used is shown below. It should also be noted that all errors in bond distances are enclosed in parentheses immediately following the quoted values.



The comparison of bond distances also requires a criterion for determining whether two bonds are different from one another. For this purpose, the following statistical expression was used:

$$\sigma = \sqrt{(e_1^2 + e_2^2)}$$

where:

- $e_1$  and  $e_2$  are the observed errors in the bonds being compared
- $\sigma$  is the error associated with the difference between the two distances

Two bond distances are considered equivalent to within 99% confidence if the difference between them does not exceed  $3\sigma$ .

### 2.3.1 2-phenyl-1,3-dioxolan-2-ylum trifluoromethanesulfonate 14b

The first 1,3-dioxolanylium cation selected for study was 14b. This compound was chosen in order to establish a point of reference for subsequent observations. The cation, 14b, is a 1,3-dioxolanylium cation with a phenyl substituent in the 2-position of the five membered ring. This cation was attractive because it had previously been prepared and was known to be stable<sup>36</sup>. Furthermore, the presence of a phenyl group offered the potential for increasing the range of substituents whose effects on the carbon-oxygen bond lengths of the five-membered ring could be studied.

#### a. The structure of 14b

The structural features of the cation 14b are displayed in the Snoopi drawing of figure 2-1. The cation consists of two rings, joined by a carbon-carbon (C-C) bond. The two rings are planar with a twist about the connecting C11-C21 bond of  $2.35^{\circ}$ .

The C-C bond distances within the phenyl group are not unusual and within the limits of experimental error close to the values of 1.38(13)Å observed in unsubstituted phenyl rings.<sup>25</sup>

The C<sup>+</sup>-O distances in this particular cation of 1.281(3)Å for the C11-O12 bond and 1.282(3)Å for the C11-O11 bond, are the same within the limits of experimental error. The C12-O11 and C13-O12 linkages have observed bond distances of 1.472(3)Å and 1.480(3)Å, respectively, which are again the same within the error limits of the measurement. The C12-

C13 internuclear distance of 1.505(5)Å is not statistically different from the value of 1.543(18)Å for a  $Csp^3-Csp^3$  bond observed in cyclopentane.<sup>25</sup>

The triflate anion which is the other component of the asymmetric unit of the complex salt sits above the five membered ring in the lattice and the closest contact between anion and cation is 2.822(3)Å between C11 of the cation and O2 of the anion.

### 2.3.2 2-(4-methoxyphenyl)-1,3-dioxolan-2-ylum hexafluoroantimonate 15b

The 1,3-dioxolanylium cation, 15b, bearing a p-methoxyphenyl substituent at position 2 of the five-membered ring was prepared in order to explore what effect the relative stability of the substituent at this position had on the structure of the dioxolanylium ring. This question was addressed because the results of the protonated benzophenone studies suggested that the overall stability of the cation should have an effect on the lengths of the carbon-oxygen bonds around the formal electron deficient carbon centre. In addition, it was hoped that any stability imparted to the carbenium ion as a result of the electron donating properties of the methoxy group would facilitate the isolation of a crystalline sample suitable for x-ray studies.

#### a. The Structure of 15b

A Snoopi drawing of the cation 15b in which some relevant bond lengths have been included is presented in figure 2-2. The dioxolanylium moiety as a whole is planar with a twist angle of 5.25° between the six

membered and five membered rings.

Consideration of the five membered ring shows it to have C<sup>+</sup>-O bond lengths of 1.293(9)Å for the C11-O11 bond and 1.292(8)Å for the C11-O12 bond, values which are the same within the limits of experimental error. The C-O distances observed are 1.474(9)Å for the C12-O11 bond and 1.466(9)Å for the C13-O12 bond.

The hexafluoroantimonate anion associated with this cation lies above the dioxolanylium ring and has a closest contact distance of 2.810(14)Å with the sp<sup>2</sup> carbon C11 of the ring. There was some disorder evident in the fluorines of the ion and these were given partial occupancy in the final structure solution.

### 2.3.3 2-(2,4-pentadienyl)-1,3-dioxolan-2-ylum hexafluoroantimonate 16b

As a further probe of the substituent effect at position 2 of the dioxolanylium ring system the cation 16b, containing a linear system of conjugated bonds was prepared. The rationale employed in the decision to study this molecule included not only its comparative usefulness as a example of a different type of conjugated substituent but also its potential as a probe for studying the extent to which charge can be delocalized within a system of linear conjugated double bonds. A previous study on a homotropylium system<sup>29</sup> provided evidence which suggested that there are limits to the ability of a conjugated system to delocalize positive charge.

The preparation of the hexafluoroantimonate salt of 16b was carried

out according to the same method used in the preparation of 15b. A suspension of silver hexafluoroantimonate in dichloromethane was prepared and to this was added a solution of the bromoester, 16a. Reaction occurred immediately to yield the cation which was recrystallized to obtain suitable crystals for an x-ray study. The  $^1\text{H}$  nmr spectrum of this cation was consistent with its structure

a. The Structure of 16b

The structure of 16b is presented in figure 2-3. The asymmetric unit consists of a linear cation and an octahedral hexafluoroantimonate anion. The results of a least squares planes calculation showed that the angle between the planes containing the five-membered ring and the plane containing the side chain is  $1.428(.164)^\circ$ , This indicates that the cation as a whole is essentially planar.

The diene exists in the relatively stable trans-trans configuration and it is evident from the geometry of the system that a favourable arrangement for the delocalization of charge through the system of  $\pi$ -bonds exists.

The C11-O11 and the C11-O12 bond lengths of  $1.288(5)\text{\AA}$  and  $1.290(5)\text{\AA}$  respectively are of comparable magnitude to the corresponding bonds in 14b and 15b.

The hexafluoroantimonate anion in this compound has a closest contact distance of  $2.870(4)\text{\AA}$  which occurs between F5 and C11 of the oxonium ion. The angle subtended at C11 by the closest fluorine atom F5

and O11 is  $80.57(21)^\circ$ . The angle subtended at C11 by F5 and O12 is  $91.03(23)^\circ$

2.3.4 2-(4-methoxyphenyl)-4-methyl-1,3-dioxolan-2-ylum  
hexachloroantimonate 17b

As was stated in chapter 1, a desire to acquire information on the effects of substitution at position 4 of the dioxolanylium ring on C-O bond distances was also one of the objectives of the present study. With this in mind, the dioxolanylium ion 17b, bearing a methyl group at position 4 (C31) of the five membered ring was prepared. It was felt that the asymmetry in the electronic distribution of the cation introduced by the presence of methyl group would have an effect on all the carbon oxygen distances within the dioxolanylium ring.

a. The Structure of 17b

An analysis of the carbenium ion, 17b, presented in figure 2-4 reveals no unusual features of the carbon oxygen bonds present in the system. The C<sup>+</sup>-O bond distances observed in this cation are  $1.274(11)\text{\AA}$  for the C11-O12 bond and  $1.291(10)\text{\AA}$  C11-O11. These bond distances are the same within the limits of experimental error suggesting that the structural asymmetry of the five-membered ring is not being reflected in the bond lengths within it. The same result is observed for the C12-O11

and C13-O12 distances which are 1.503(13)Å and 1.476(13)Å, the C13 carbon being the asymmetric carbon centre bearing the methyl group.

The C13-C131 bond distance observed in this carbenium ion is 1.319(36)Å. This bond is extremely short for a  $Csp^3-sp^3$  bond and the error associated with it is very large. This unusual bond distance is attributed to the disorder in this system caused by the presence of a pseudo-mirror plane which contains, with the exception of C131, all the carbon and oxygen atoms of both ring systems.

The twist angle between the dioxolanylium ring and the phenyl ring is 1.430°. The values of the bond distances around the phenyl ring do not suggest a marked deviation from the  $D_{6h}$  symmetry of benzene and the length of the C11-C21 bond connecting the two rings, at 1.441Å, does not suggest that there is significant delocalization of positive charge into the aromatic ring.

### 2.3.5 2-(4-methoxyphenyl)-4,4-dimethyl-1,3-dioxolanyl-2-ylum hexachloroantimonate 18b

In order to further study the effect of alkyl substitution at position 4 of the dioxolanylium ring system, the dioxolanylium ion, 18b, was prepared. This ion bears gem dimethyl groups at carbon 4 of the five membered ring. The presence of the two methyl substituents was expected to demonstrate more clearly (cf. structure 17b) the effects of methyl substitution and to provide further information about the nature of the

bond reorganization which occurs around charge bearing oxygens.

a. The Structure of 18b

The carbenium ion, 18b, shown in figure 2-5, is part of an asymmetric unit made up of a dioxolanylium cation and an octahedral hexafluoroantimonate anion. The angle of twist between the two constituent ring systems of the cation is at  $8.976^\circ$  the largest observed in any of the 2-aryl-1,3-dioxolan-2-ylium systems surveyed. The bond distances around the phenyl ring are, within the limits of experimental error, the same as those observed in benzene.

The bond distances observed for the para-substituted methoxy group suggest the absence of its participation in resonance mediated charge stabilization. The values of  $1.435(19)\text{\AA}$  and  $1.445(20)\text{\AA}$  for the C24-O31 and O31-C31 bonds respectively suggest that they are akin to the ether linkages observed in neutral p-substituted benzenes<sup>25</sup>, however this could in part be due to the very large errors in the structure which make comparisons with other structures difficult.

The bond distances observed in the five-membered ring follow the trend observed for the 4-methyl substituted cation, 17b, discussed above. The C<sup>+</sup>-O bond distances are  $1.286(15)\text{\AA}$  for the C11-O11 bond and  $1.306(16)\text{\AA}$  for the C11-O12 bond. The observed C12-O11 distance was  $1.486(17)\text{\AA}$  while the C13-O12 distance was observed to be  $1.546(15)\text{\AA}$ . Again, the magnitude of the errors in this structure makes the comparison of bond distances difficult but the value of  $2.6\sigma$  calculated for the



difference between the C12-O11 and C13-O12 bonds suggests that the asymmetry of the two environments may be reflected in their bond distances.

## CHAPTER 3

### INTERPRETIVE DISCUSSION

#### 3.1 Comparative Analysis of the 1,3-Dioxolan-2-Ylium Cations 14b-18b

The following section presents an analysis of the gross structural features of the dioxolanylium cations studied in this work. It is an examination of the effects of systematic substituent change at positions 2 and 4 of the dioxolanylium ring on the bond distances observed within this ring. These changes in turn have implications for the description of the charge distribution in these ions and on the relative importance of the resonance structures used to describe the protonated carbonyl group.

##### 3.1.1 Structural Features of Substituents at Position 2

The stabilization of a carbenium ion by the delocalization of positive charge throughout a network of pi-type bonds is an established concept. It was therefore of interest to observe whether or not this form of stabilization was reflected in the bond lengths of those ions bearing substituents capable of pi-type interaction with the formally charged carbon atom.

The first of the dioxolanylium ion studied, 14b, was found to have a twist angle between the phenyl ring and the dioxolanylium ring of  $2.35^{\circ}$ . Such a small angle of twist suggests that this system is geometrically suited to stabilization by conjugation between the electron deficient

carbon atom and the electron rich phenyl ring. A comparison of the observed C11-C21 bond distance of 1.442(3)Å to the bond distance of 1.487(12)Å observed for the Csp<sup>2</sup>-Car bond in aryl esters<sup>25</sup> indicates that the bond distances are different. This result suggests that a contraction of the C11-C21 bond relative to the value observed in the neutral species has occurred and supports the possibility of conjugative stabilization.

The carbenium ion, 15b, would, according to currently held views, be expected to be more stable than 14b owing to the presence of the electron donating methoxy substituent in the para position of the phenyl ring. This ion would also be expected to stabilize its positive charge through a conjugative interaction.

An examination of the bond distances in the phenyl ring of this molecule yields evidence for the distortion of the ring away from the D<sub>6h</sub> symmetry of benzene. The bonds, C21-C22, C21-C26, C24-C23, and C24-C25 show evidence of lengthening. A relative contraction in bond distance is observed for the C22-C23, and C25-C26 bonds. The calculation of an average bond distance for those bonds which show evidence of lengthening yields a value of 1.405(2)Å. The observed bond distance of the C22-C23 and C25-C26 bonds is 1.350(10)Å. When the statistical test described in Chapter 2 is applied to determine whether the two sets of bonds are significantly different from one another, a value of 5.3σ is obtained. This implies that the bond distances compared are different. This suggests the possibility that the phenyl ring in this structure is beginning to exhibit the D<sub>2h</sub> symmetry of a quinoid structure. If this

were the case, both the C24-O21 bond and the C11-C21 bonds would be expected to have bond lengths which were shorter than those observed in neutral systems. A comparison of the C11-C21 bond distance of 1.414(9)Å to the 1.487(12)Å of the  $C_{sp^2}$ -Car bond found in aryl esters<sup>25</sup> reveals that the C11-C21 bond is shorter than the corresponding bond in the neutral species. The bond angle subtended at the methoxy oxygen by the carbon atom, C24, of the phenyl ring and the carbon atom of the methyl ether, C31, is 120(6)<sup>o</sup> and further suggests that the geometry of the methoxy substituent is of the quinoid form. However, a comparison of the C24-O21 bond distance of 1.348(13)Å with the 1.370(11)Å Car-O bond of aryl alkyl ethers<sup>25</sup> reveals that they are the same within the limits of experimental error.

The observations discussed above hint at the possibility that the p-methoxyphenyl substituent contributes to the stabilization of the oxonium ion by engaging in a conjugative interaction with the electron deficient carbon centre C11. However, in the absence of a contraction of the C24-O21 bond distance, this cannot be stated with certainty.

Due to their similarity to 15b, the carbenium ions 17b and 18b, both of which bear p-methoxyphenyl substituents at the 2-position of the dioxolanylium ring may reasonably be expected to show similar trends in the bond lengths of their phenyl substituents. However, it was not possible to make statistically meaningful comparisons of these bond distances due to the relatively large errors associated with the bond measurements in these structures.

The conjugated polyene of 16b represents the first crystal structure of a 1,3-dioxolan-2-ylum ion bearing a linear system of conjugated bonds at position 2 of the five-membered ring. The system of conjugated bonds offers the potential for stabilization of the carbenium ion through pi-bond resonance. The planarity of the entire system provides a geometry which allows for the occurrence of extensive delocalization. However, this expectation is not supported by the observed bond distances.

Within the polyene chain, a system of alternating double and single bonds exists. This points to the limited participation of the linear  $\pi$ -system in the delocalization of charge within the carbon framework. There is structural evidence for some short range interaction between the electron deficient carbon, C11, and the polyene chain. This is illustrated by a comparison of the lengths of the  $C_{sp^2}=sp^2$  bonds [C21-C31 and C41-C51] and the  $C_{sp^2}-sp^2$  bonds [C11-C21, C31-C41, and C51-C61], the results of which are shown in table 3-1.

Table 3-1

Comparison of Bond Distances in 16b to Literature Values<sup>25</sup>

<u>Bond</u>	<u>Bond Distance(A)</u>	<u>Literature Values</u>	<u>Value of <math>\sigma</math></u>
C11-C21	1.417(5)	1.488(14)	4.8
C31-C41	1.435(5)	1.455(11)	1.7
C51-C61	1.482(6)	1.503(11)	1.7
C21-C31	1.349(6)	1.340(13)	0.6
C41-C51	1.324(6)	1.330(14)	0.4

The table above compares the bond distances of the  $Csp^2-sp^2$  double and single bonds of 16b to the literature values<sup>25</sup> of the bonds they most closely resemble in uncharged systems. The results reveal that while the only statistically significant difference occurs for bond C11-C21, there is a trend in which smaller differences between comparable bond distances of the neutral and protonated species are observed as the distance from the cationic centre increases.

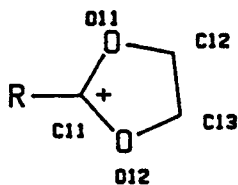
### 3.1.2 The Effect of Substitution on the Dioxolanylium System

Table 3-2 provides a summary of the bond lengths for the five cations prepared for this work and also includes relevant bond distances for the two literature examples of dioxolanylium cations 12 and 13 (Chapter 1) for which x-ray structure data is available.

Consider the C11-O11 and the C11-O12 bonds of the compounds in table 3-1. The average bond distance of a  $Csp^2-O$  bond in aryl esters is 1.337(13)Å and for the  $Csp^2=O$  bond of aryl esters, the average distance is 1.209(9)Å.<sup>25</sup> The expected effect of creating a charge deficient centre at position C11 [by the acid-mediated intramolecular alkylation of a suitable ester to create a 1,3-dioxolan-2-ylum system] would be the lengthening of the  $Csp^2=O$  bond and the contraction of the  $Csp^2-O$  bond. This was indeed the case with each of the cations studied (14b - 18b) and both literature examples (12 and 13), for which  $C^+-O$  bond distances intermediate to those of the  $Csp^2-O$  and  $Csp^2=O$  bonds were observed.

TABLE 3-2

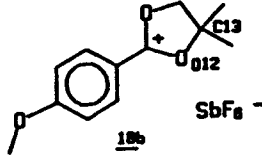
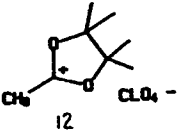
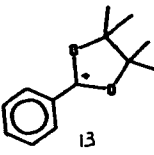
1,3-Dioxolan-2-Ylium five-membered ring Bond Distances (Å)



Bond	R-C11	C11-O11	O11-C12	C12-C13
Compound		C11-O12	O12-C13	
 <u>14b</u>	1.442(3)	1.282(3)	1.472(3)	1.505(5)
		1.281(3)	1.480(3)	
 <u>15b</u>	1.414(9)	1.293(9)	1.474(9)	1.503(11)
		1.292(8)	1.466(9)	
 <u>16b</u>	1.417(5)	1.288(5)	1.472(5)	1.515(7)
		1.290(5)	1.469(5)	
 <u>17b</u>	1.441(14)	1.291(10)	1.476(13)	1.567(14)
		1.274(11)	1.503(13)	

TABLE 3-2 cont'd

## 1,3-Dioxolan-2-Ylium five-membered ring Bond Distances (Å)

Compound	Bond	R-C11	C11-O11	O11- C12	C12-C13
			C11-O12	O12-C13	
 10b		1.409(17)	1.286(15)	1.416(17)	1.574(19)
			1.306(16)	1.546(15)	
 12		1.504(18)	1.277(18)	1.521(15)	1.566(10)
			1.241(2)	1.520(19)	
 13		1.47(2)	1.29(1)	1.52(1)	1.56(2)
			1.29(1)	1.52(1)	



The C11-011 and C11-012 bonds of each 1,3-dioxolan-2-ylum ion studied were compared to determine whether or not statistically relevant differences in length (i.e.  $>3\sigma$ ) existed between any like pair of bonds. This analysis revealed that none of the like pairs of bonds compared, were significantly different in length from one another. This would suggest that the C11-011 and C11-012 bond lengths were not overly sensitive to changes in substitution at position 2 of the five-membered ring.

It is noteworthy to emphasize that the comparison described in the paragraph above includes the compounds 15b, 17b and 18b all of which bear the p-methoxyphenyl substituent at position 2 of the dioxolanylium ring. As previously mentioned these ions differ in their substitution at position 4 (C31) of the dioxolanylium ring. The bond comparison analysis shows that while the values of  $\sigma$ , representing the degree of difference in bond lengths between the compounds, is slightly larger for the C11-012 bonds than it is for the C11-011 bonds, in no instance is it large enough to suggest that the pairs of bonds compared differ in length from one another. This result suggests that the C11-011 and the C11-012 bond distances in these systems are not sensitive to changes in methyl substitution at position 4 of the five-membered ring. This was somewhat unexpected as measurable changes in the C11-012 bond distance in particular were predicted based on the expectation that more positive charge would be concentrated at position C13 as the level of methyl substitution at that position was increased. Again, it should be noted

that the large errors associated with the bond distances in both 17b and 18b may make it more difficult to observe differences between the values compared.

The O11-C12 and O12-C13 bond distances are expected to be good indicators of the nature of the gross bond reorganization occurring in these systems because they are the linkages between the "carbonyl" oxygens and the adjacent alkyl groups described by the resonance structures of equation 1-2. In addition, these bonds were observed to be unusually long in the literature examples 12 and 13.

In the five carbenium ions studied, these bonds are observed to have begun a lengthening away from the value of 1.42(3)Å observed in 1,3-dioxolane.<sup>39</sup> The O11-C12 bonds of 14b, 15b, and 16b are observed to have the same bond lengths, lengths of 1.472(3)Å, 1.474(9)Å, and 1.472(5)Å respectively.

Similarly, the values of the O12-C13 bond for the three compounds 14b, 15b, and 16b are 1.480(3)Å, 1.466(9)Å and 1.469(5)Å respectively. Again, the dimensions of the three bonds are the same within the error limits of the measurement and are beginning to lengthen away from the 1.42(3)Å of dioxolane.<sup>39</sup>

In addition, as would be expected based on the symmetry of the system, the O11-C12 and O12-C13 bond distances of each ion 14b, 15b, and 16b are the same within the limits of experimental error.

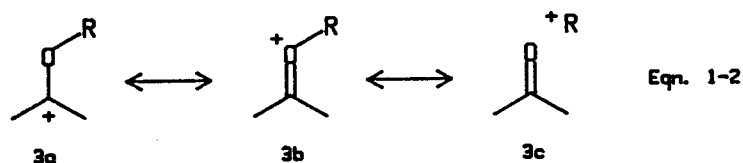
In stark contrast to the ions in which no substituent exists at position 3 or 4 of the five-membered ring, carbenium ions 17b and 18b

display disparities in the bond lengths of their dioxolanylium ring which arise from the asymmetry of their ring systems. The O12-C13 bond distances of the three methoxyphenyl bearing compounds, 15b, 17b, and 18b are 1.466(9)Å, 1.503(13)Å, and 1.546(15)Å respectively. A statistical comparison of the O12-C13 bond distances of 17b and 18b yields a value for  $\sigma$  of 2.2. A similar comparison of the O12-C13 bonds of 15b and 18b yields a value of  $4.6\sigma$ . These results suggest that an increase in the length of the O12-C13 bond parallels the increasing degree of methyl group substitution at C13. Again, it must be noted that the poor quality of the structures 17b and 18b may materially affect the observations on which this conclusion has been drawn.

The effects of the poor quality structures may be tempered in this instance by analyzing the difference in the bond lengths of the O12-C13 bonds in structures 13 and 14b. The length of this bond in 13 is 1.52(1)Å and the corresponding bond distance in 14b is 1.480(3)Å. These two bonds are statistically different from one another ( $\sigma=3.8$ ) and this result supports the contention that the increase in methyl substitution at position C13 of the five-membered ring is accompanied by an increase in the O12-C13 bond distance.

These results provide evidence in support of the hypothesis that an alkylated (or protonated) carbonyl group can be described by a resonance structure in which a significant amount of charge resides on the alkylating species (structure 3c, equation 1-2). This also implies that in the limit where a substituent capable of fully stabilizing the positive

charge on the molecular fragment exists at C13 of this system, an extreme lengthening of the O12-C13 distance to the point where the existence of a covalent bond is questionable will be observed.



A further implication of the trend observed in the O12-C13 bond distances of 15b, 17b and 18b is that it provides static evidence for a dynamic process, specifically, a nucleophilic substitution reaction in which a carbonyl group acts as an incoming nucleophile. The observed changes in the geometry around the carbon to which the nucleophile is added are subtle! This is because the three structures only cover a small distance along the reaction coordinate and do not allow the observation of large structural changes. However, there is evidence of geometric reorganization. As one moves from 15b with no methyl substituent at position 4 of the five-membered ring to the monomethyl cation, 17b, to the dimethyl substituted cation, 18b, one observes a reduction in the value of the C12-C13-O12 bond angle from  $103.20(0.60)^\circ$  to  $100.58(0.80)^\circ$  to  $99.85(0.95)^\circ$ . When considered with the value of  $108^\circ$  observed for the

equivalent angle in 1,3-dioxolan, this provides supporting evidence of the change in geometry around C13 towards a trigonal planar configuration. In other words, the three structures collectively, allow one to observe the latter stages of the approach of the nucleophile to the electrophilic site.

### 3.2 Concluding Remarks

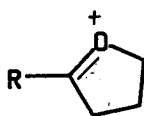
The primary objective of this thesis was to probe the effects of systematic substituent changes on the carbon-oxygen bond distances of a series of O-substituted ions. While this comparison was made more difficult by the poor quality of structures 17b and 18b which made the results of bond distance comparisons between these and other cations less reliable there is, however sufficient data to suggest that this study using the 1,3-dioxolan-2-ylum model system provides evidence of changes in the charge distribution of the series of ions studied. Such change was manifested in the form of differences in the bond distances between like-bonds in the series of ions studied. Evidence of this phenomenon was most apparent from the comparison of carbon-oxygen bond distances between the three methoxyphenyl substituted ions (15b, 17b, and 18b) and between the phenyl substituted ions 13 and 14b. There is clearly a systematic increase in the separation of the "carbonyl" oxygen and the adjacent methyl-bearing locus as the level of methyl substitution is increased. Such a systematic change supports the hypothesis put forward in this thesis that the protonation or alkylation of a carbonyl group will result

in a structure which can best be described by resonance structures in which charge is shared with adjacent centres and not concentrated on the oxygen atom.

This work also reveals that the substituent changes made at position 2 of the dioxolanylium ring do not have a significant impact on the bond distances observed within this ring. Evidence for this conclusion is provided by the equivalence of the dioxolanylium ring bond distances which persists as the substituent at position 2 was changed from phenyl (14b) to p-methoxyphenyl (15b) to 2,4-pentadienyl (16b).

This work also resulted in the first x-ray crystal structure determination of a dioxolanylium cation bearing a linear system of conjugated double bonds at position 2 of the dioxolanylium ring.

Although the true nature of the charge distribution in O-substituted carbenium ions was revealed to some extent by the study of the 1,3-dioxolan-2-ylum system, future work in this area would probably yield more unequivocal results if a system containing only one oxygen adjacent to the Csp<sup>2</sup> carbon was used. A good model for such an investigation would be a series of methyl substituted oxolan-2-ylum ions, 19.



As these have only a single oxygen atom capable of stabilizing the positive charge, one would anticipate the observation of more profound changes in the bond distances around oxygen as a series of systematic substituent changes were made.

## CHAPTER 4

### EXPERIMENTAL METHODS

#### 4.1 Instrumental Techniques

<sup>1</sup>H NMR spectra were obtained on Varian EM-390, Bruker WM-250, and Bruker WM-500 spectrometers. Spectra recorded on the Varian instrument were referenced with TMS; those measured on the Bruker instrument were referenced using solvent signals. All spectra were run at room temperature in deuterated solvents.

X-ray diffraction data for the crystals studied was collected on either a Syntex P2<sub>1</sub> or Nicolet P3 automatic diffractometer equipped with a low temperature apparatus. All intensity measurements were made at low temperature (-65°C) with MOK<sub>α</sub> radiation (λ=0.71069Å).

Mass spectra were obtained on a VG-ZAB-E mass spectrometer operating at an ionization potential of 70eV and a source temperature of 200°C.

All calculations related to the solution and refinement of the crystal structures were performed on either a Control Data Cyber computer or on a Digital Equipment Corporation VAX-8600.

#### 4.2 Purification of Solvents

Ether was freshly prepared as needed by distillation under a nitrogen atmosphere from a lithium aluminum hydride/ether suspension.

CH<sub>2</sub>Cl<sub>2</sub> and CH<sub>3</sub>CN were refluxed over phosphorus pentoxide and



distilled under a nitrogen atmosphere prior to their use. All dried solvents were stored in a glove bag which was continuously purged with dry nitrogen.

### 4.3 Syntheses

#### a $\beta$ -hydroxyethyl benzoate 14a

This compound was prepared by the modified method of Nanasawa et al.<sup>40</sup> To a mixture of benzoic acid (6.35g) and p-toluenesulfonic acid (0.86g) in benzene (50mL), was added ethylene glycol (7.4mL) and the resulting mixture was refluxed with stirring under a nitrogen atmosphere in a Dean and Stark apparatus for 1 hour. The distillate was removed and the mixture was treated with further ethylene glycol (7.4mL) and refluxed for a further 2 hours. The cooled mixture was poured onto ice brine and ether extracted. The organic layer was washed with 10% NaHCO<sub>3</sub> and dried over anhydrous MgSO<sub>4</sub>. Removal of the ether on a rotary evaporator yielded a yellow liquid which upon distillation gave a clear colourless liquid (b.p. 100°C at 0.5mm Hg). High res. M.S.(m/e):M+1 obsd: 167.0710, M+1 calcd: 167.0708. Nmr appears in table 4-1.

#### b $\beta$ -bromoethyl-4-methoxybenzoate 15a

The ester, 15a, was prepared according to the modified method of Forde-Moore.<sup>41</sup> A mixture of anisoyl chloride (10g) and 2-bromoethanol (7.50g) was added to a round bottomed flask outfitted with a drying tube

and condenser. The mixture was stirred and heated at 80°C for 15 hours. Upon completion of the reaction, the contents of the flask were extracted into ether (25mL) and the extract washed with water (3x10mL). This was followed by washing with a 10% NaHCO<sub>3</sub> solution (3x10mL) after which the ether solution was dried over anhydrous MgSO<sub>4</sub>. The removal of the ether by rotary evaporator yielded a brown liquid. Subsequent distillation at reduced pressure yielded a pale yellow liquid (b.p. 103°C at 0.5mm Hg). High res. M.S.(m/e):M<sup>+</sup> obsd: 257.9901, M<sup>+</sup> calcd: 257.9892. Nmr(table 4-1)

c β-bromoethyl-2,4-pentadienoate 16a

The ester, 16a, was prepared using a modified version of the method of Rehberg.<sup>42</sup> To a solution of 2,4-pentadienoic acid (8.97g) in benzene (50mL) was added 2-bromoethanol (15g) and p-toluenesulfonic acid (1.52g). The resulting mixture was refluxed for 6 hours at the end of which it was cooled and extracted into ether. The extract was washed first with water (3x25mL) and then with a 10% NaHCO<sub>3</sub> solution (3x25mL). This was followed by drying over MgSO<sub>4</sub> and removal of the solvent on the rotary evaporator and the distillation of the resulting oil to obtain the product as a pale yellow liquid (b.p. 78°C at 0.5mm Hg). High res. M.S.(m/e):M<sup>+</sup> obsd: 217.9947 M<sup>+</sup> calcd: 217.9942. Nmr (table 4-1)

d 1-methyl-2-bromopropyl-4-methoxybenzoate 17a

This compound was prepared in a manner similar to that employed for 15a above.<sup>41</sup> A mixture of anisoyl chloride (5g) and 1-bromo-2-propanol

(4.5g) was refluxed for 17 hours at 72°C. The reaction product was then distilled with no cooling water to yield a clear colourless liquid (the fraction which distilled in the range 60°C-70°C at 0.5mm Hg was collected). High res. M.S.(m/e):M<sup>+</sup> obsd: 272.0051, M<sup>+</sup> calcd: 272.0048. Nmr(table4-1)

e 2-propen-4-methoxybenzoate 18a

The preparation of the ester, 18a, was effected using a modified method of Blake.<sup>43</sup> Anisoyl chloride (5g in 20ml benzene) was added dropwise to 2-methyl-2-propen-1-ol (2.83g) and pyridine (3.11g) in benzene (150mL) at room temperature. The reaction mixture was brought to gentle reflux and heated for 6 hours. Upon cooling, the pyridinium hydrochloride, formed during the course of the reaction was filtered off and ether added. The ether/benzene solution was washed thoroughly with water and a 10% NaHCO<sub>3</sub> solution, dried over MgSO<sub>4</sub> and the solvent removed on the rotary evaporator to yield a clear colourless liquid. Distillation gave a pure sample (by nmr) which was clear colourless liquid (b.p. 60°C at 0.5mm Hg). High res. M.S.(m/e):M<sup>+</sup> obsd: 206.0953, M<sup>+</sup> calcd: 206.0943. Nmr (table 4-1).

f 2-phenyl-1,3-dioxolan-2-ylum trifluoromethanesulfonate 14b

The triflate salt, 14b, was prepared according to the method of Blackburn.<sup>35</sup> The reaction was conducted in a vessel consisting of two limbs separated by a porous sintered glass frit. A solution of the

ester, 14a, (0.50g) in  $\text{CH}_2\text{Cl}_2$  (5ml) was introduced into one limb of the flask which had been flame-dried on a vacuum line prior to use. The arm of the flask containing the ester solution was cooled to  $-78^\circ\text{C}$  in a dry ice/acetone bath and at this point, triflic anhydride (659 $\mu\text{l}$ ) in  $\text{CH}_2\text{Cl}_2$  (2ml) was added to the other arm. The contents of both arms of the flask were allowed to mix and this mixture was slowly warmed to room temperature. The addition of ether resulted in the precipitation of the triflate salt. The entire process as described to this point was carried out under a dry nitrogen atmosphere in a glove bag. The precipitate was redissolved in  $\text{CH}_3\text{CN}$  after removal of the  $\text{CH}_2\text{Cl}_2$  and ether by decantation and kept at  $-15^\circ\text{C}$  overnight during the course of which fresh ether was slowly distilled into the solution by vapour diffusion. In this manner, well-formed colourless crystals were obtained which proved suitable for x-ray diffraction studies. NMR spectrum given in table 4-1.

g 2-(4-methoxyphenyl)-1,3-dioxolan-2-ylum hexafluoroantimonate 15b

This carbenium ion salt was prepared using the method of Meerwein.<sup>36</sup> In a glove bag which was continuously purged with nitrogen, a solution of the ester, 15a, (0.50g in 2mL  $\text{CH}_2\text{Cl}_2$ ) was added to an aluminum foil covered vial containing a mixture of  $\text{AgSbF}_6$  (0.66g) and  $\text{CH}_2\text{Cl}_2$  (2mL). An instantaneous reaction occurred to yield  $\text{AgBr}$  and a solution containing the carbenium ion salt. The  $\text{AgBr}$  was removed by gravity filtration and freshly distilled dry ether was added to the filtrate until precipitation of the salt ensued. The ether and  $\text{CH}_2\text{Cl}_2$  were decanted off and the salt

was redissolved in dry  $\text{CH}_3\text{CN}$ . This solution was placed in a freezer at  $-15^\circ\text{C}$  and fresh ether was added by vapour diffusion. This resulted in the formation of colourless rectangular prisms of suitable quality for an x-ray diffraction experiment. NMR spectrum given in table 4-1.

h 2-(2,4-pentadienyl)-1,3-dioxolan-2-ylum hexafluoroantimonate 16b

The cation, 16b, was prepared in a manner analogous to the preparation of 15b above. To a mixture of  $\text{AgSbF}_6$  (0.39g) and  $\text{CH}_2\text{Cl}_2$  (2mL) was added a solution of the ester, 16a, (0.25g in 2mL  $\text{CH}_2\text{Cl}_2$ ). The precipitate which formed was collected by gravity filtration and washed with a small quantity of dry  $\text{CH}_3\text{CN}$  (2mL). The washings were added to the  $\text{CH}_2\text{Cl}_2$  solution and to the resulting solution was added sufficient diethyl ether to prompt the precipitation of the salt. After removal of the solvent mixture by decantation, the precipitate was redissolved in fresh  $\text{CH}_3\text{CN}$  and ether distilled into the solution by vapour diffusion. The crystals thus formed were colourless plates, well suited for use in the collection of x-ray data. NMR spectrum given in table 4-1.

i 2-(4-methoxyphenyl)-4-methyl-1,3-dioxolan-2-ylum hexafluoroantimonate 17b

This salt was made using the same approach employed in the preparation of the salts, 15b and 16b above. A solution of the ester, 17a, (0.25g in  $\text{CH}_2\text{Cl}_2$ ) was added to a mixture of  $\text{AgSbF}_6$  (0.32g) and  $\text{CH}_2\text{Cl}_2$  (2mL). The  $\text{AgBr}$  formed during the course of the reaction was

removed by filtration and precipitation of the carbenium ion salt was effected from the filtrate by the addition of dry diethyl ether. The precipitate was redissolved in  $\text{CH}_2\text{Cl}_2$  placed in a freezer at  $-15^\circ\text{C}$  and recrystallization expedited by the vapour diffusion of fresh ether into the solution. The resulting crystals were colourless rectangular prisms.

j 2-(4-methoxyphenyl)-4,4-dimethyl-1,3-dioxolan-2-ylum  
hexafluoroantimonate 18b

This compound was prepared according to a modified method of Larsen<sup>44</sup> and was carried out under a nitrogen atmosphere in a glove bag. A quantity of the ester, 18a, (0.41g) dissolved in  $\text{CH}_2\text{Cl}_2$  (4mL) was placed in a Schlenck tube and cooled to  $-78^\circ\text{C}$  in a dry ice/acetone bath. To this solution was added a mixture of cold ( $-15^\circ\text{C}$ )  $\text{HSbF}_6$  (157 $\mu\text{L}$ ) in  $\text{CH}_2\text{Cl}_2$  (2mL). The tube and its contents were shaken vigorously and left at  $-78^\circ\text{C}$  for  $1\frac{1}{2}$  hours. Dry ether (5mL) was then added to the solution and it was placed in a tightly sealed container and stored in a freezer at  $-15^\circ\text{C}$ . Crystallization ensued to yield colourless rectangular prisms suitable for analysis by x-ray diffraction.

TABLE 4-1

<sup>1</sup>H NMR Chemical Shifts for Esters 14a-18a and Salt 16b

<u>Compound</u>	<u>Ester protons</u>	<u>Aromatic</u>	<u>Other protons</u>
14a	α3.65(t) β3.14(t)	7.3(m) 6.6(m)	OH 2.6(s)
15a	α4.6(t) β3.6(t)	6.9(d) 8.1(d)	OCH <sub>3</sub> 3.9(s)
16a	α4.4(t) β3.5(t)	7.3(m) 6(m)	CH <sub>3</sub> 1.8(d)
17a	α5.2(q) β3.5(d)	6.9(m) 7.8(m)	OCH <sub>3</sub> 3.8(s)
18a	α4.7(s)	8.1(m) 7.5(m) 5(d)	OCH <sub>3</sub> 3.7(s) CH <sub>3</sub> 1.9(s)

<u>Compound</u>	<u>Ring protons</u>	<u>Vinyl</u>	<u>Other protons</u>
16b	5.31(s)	8.0(q) 6.9(m) 6.6(m) 6.1(m)	CH <sub>3</sub> 2.1(m)

s = singlet, d = doublet, t = triplet, q=quartet, m = multiplet

\* all spectra were run in CD<sub>2</sub>Cl<sub>2</sub>

#### 4.4 Crystal Structure Determinations

For all of the crystals studied, the same procedures were employed in the handling, selection, sealing, and other preliminary processes which precede intensity data collection.

##### i Crystal selection and handling

All crystals studied were prepared and handled under a dry nitrogen atmosphere during the entire course of the experiments. Once crystals which appeared to be of suitable size and quality were obtained, they were transferred to a Vacuum/ Atmospheres Company HE 43-2 DRI-LAB equipped with a VAC DC-882 DRI-COLD storage unit and a Bausch and Lomb Stereo Zoom 7 microscope for mounting and sealing. Crystals which best approximated cubes of dimensions .3mmx.3mmx.3mm were chosen for study. In some instances, it was necessary to cut the crystals with a razor blade in order to obtain samples of suitable size and shape. Crystals chosen for study were mounted and sealed in Lindemann glass capillary tubes of diameter 0.3mm.

##### ii Data collection and structure solution

In the case of all five carbenium ion salts for which crystal structures were determined, Buerger-type precession photography was used to determine potential space groups and to establish approximate unit cell dimensions prior to mounting the crystal specimens on an automatic



diffractometer.

a Structure 14b

Unit cell parameters for 14b were obtained from a least squares fit of  $\chi$ ,  $\phi$ , and  $2\theta$  for 15 reflections in the range  $20^\circ < 2\theta < 24^\circ$  recorded on a Syntex P2<sub>1</sub> diffractometer using MoK $\alpha$  radiation ( $\lambda = 0.71069 \text{ \AA}$ ). This was followed by the collection of reflection intensities on the same diffractometer using a coupled  $\theta$  (crystal) -  $2\theta$  (counter) scan.

Upon the completion of data collection, corrections were made for Lorentz and polarization effects and a set of scaled intensities were obtained. The structure was solved by direct methods and refined using a full-matrix least squares routine of the program SHELX.<sup>38</sup> Temperature factors of all non-hydrogen atoms were made anisotropic and further refined by minimizing  $\sum w(F_o - F_c)^2$  until the maximum shift/error was  $< 0.20$ . A complete listing of all the pertinent information relating to the final structure solution is presented in table 4-1. Tables of non-hydrogen atom positions, hydrogen atom positions and anisotropic temperature factors appear in appendix 1.

b Structure 15b

The unit cell parameters for 15b were established by a least squares fit of  $\chi$ ,  $\phi$ , and  $2\theta$  for 15 reflections in the range  $21^\circ < 2\theta < 28^\circ$  recorded on a Nicolet P3 automatic diffractometer. The collection of a set of reflection intensities was carried out on the same

diffractometer using a coupled  $\theta$  (crystal)  $2\theta$  (counter) scan.

A correction was made to the collected intensities to account for Lorentz and polarization effects and the data scaled. This was followed by a three-dimensional Patterson synthesis using the program SHELX which yielded the position of the antimony atom. A least squares refinement utilizing SHELX was carried out to obtain the positions of all non-hydrogen atoms.

The solution obtained incorporated a disordered hexafluoroantimonate ion in which the fluorine atoms were assigned partial occupancy and were left isotropic. All other non-hydrogen atoms including the antimony of the anion were assigned anisotropic temperature factors, a weighting scheme was introduced and the structure was further refined until the maximum shift/error was  $< 0.20$  at which point the refinement was terminated. Details of the data collection and final structure solution are summarized in table 4-2 and listings of non-hydrogen atom positions, hydrogen atom positions and anisotropic temperature factors appear in appendix 1.

c Structure 16b

Data collection for 16b was initiated with the determination of unit cell parameters. This was accomplished by performing a least squares fit of  $\chi$ ,  $\phi$ , and  $2\theta$  for 15 reflections in the range  $21^\circ < 2\theta < 26^\circ$ . Once, unit cell dimensions had been obtained, a set of reflection intensities were measured and recorded with a Nicolet P3 diffractometer using the same method of data collection described for 14b and 15b.

Data reduction was carried out with the program XTAL.<sup>45</sup> This yielded a set of scaled structure factors, corrected for Lorentz and polarization effects. A Patterson synthesis was used to determine the position of the antimony atom present in the counterion and successive applications of a full-matrix least squares refinement coupled with the use of difference maps allowed determination of the positions of all the remaining non-hydrogen atoms. All non-hydrogen atoms were assigned anisotropic temperature factors and hydrogen atoms revealed by an electron density difference map were included and their positions fixed. A weighting scheme was introduced and the structure refined to a maximum shift/error of < 0.20. The Patterson synthesis was calculated using the SHELXS automatic structure solution program and subsequent refinement cycles were all accomplished using the program SHELX. A list of parameter values associated with the final structure solution is presented in table 4-3. Non-hydrogen atom positions, hydrogen atom positions, and anisotropic temperature factors have been tabulated and appear in appendix 1.

d Structure 17b

Accurate unit cell parameters were established for 17b by a least squares fit of  $\chi$ ,  $\phi$ , and  $2\theta$  for 15 reflections within the range  $22^\circ < 2\theta < 34^\circ$  recorded on a Syntex P2<sub>1</sub> diffractometer. Once this the unit cell size had been determined, a set of reflection intensities were measured and recorded on the same diffractometer.

The data was scaled and corrected for Lorentz and polarization effects using the program XTAL. The program SHELX was then invoked and

used for all subsequent calculations. The position of the antimony atom present in the anion was established using a three-dimensional Patterson synthesis. The remaining non-hydrogen atom positions were determined through the use of several cycles of full-matrix least squares refinements in conjunction with electron density difference maps. As in the case of 15b described above the fluorines of the hexafluoroantimonate anion were found to be disordered and an appropriate model was invoked in which the anion exists in two different orientations and the fluorine atoms of each orientation are assigned partial occupancies. All other non-hydrogen atoms in the structure were made anisotropic. All the hydrogen atoms could not be located from a difference map so only those which were present were included in the final stages of the refinement and these were given fixed positions and temperature factors. A weighting scheme was implemented and the refinement continued until the maximum shift/error was  $< 0.20$ . The details of the final structure solution are summarized in table 4-4 and a listing of non-hydrogen atom positions, hydrogen atom positions and temperature factors appear in appendix 1.

e Structure 18b

The unit cell parameters for 18b were determined from a least squares fit of  $\chi$ ,  $\phi$ , and  $2\theta$  for 15 reflections in the range  $19^\circ < 2\theta < 30^\circ$  recorded on a Nicolet P3 diffractometer. The reflection intensity data was collected on the same instrument using the same procedure applied to the structures previously discussed.

Scaling of the data and correction for Lorentz and polarization effects was accomplished with the program XTAL. The position of the heavy atom, Sb, was determined from a Patterson synthesis generated using SHELX and the position of all non-hydrogen atoms was determined by several cycles of least squares refinements conducted using the same program. It was not possible to refine the structure with all the non-hydrogen atoms anisotropic, so in this instance, only the antimony was given anisotropic temperature factors. Not all the hydrogen atoms were located and those which could be found were given fixed positions and temperature factors. The refinement was continued with a weighting scheme until the maximum shift/error was  $< 0.5$ . Table 4-5 provides a listing of some parameters related to the final structure solution and a list of non-hydrogen atom positions and hydrogen atom positions is presented in appendix 1.

Table 4-2 Crystal Data for 14b


---

Compound name	2-phenyl-1,3-dioxolan-2-ylum trifluoromethanesulfonate	
Compound formula	$C_9H_9O_2^+ CF_3SO_3^-$	
Formula weight	298.23	
Crystal shape and size (mm)	cylinder; r=0.15, l=0.5	
Systematic absences	hkl, h+k=2n+1; hol, h,l=2n+1; Okl, k=2n+1 hk0, h+k=2n+1; h00, h=2n+1; 00l, l=2n+1	
Space group	C2/c (No.15)	
Diffractometer	Syntex P2 <sub>1</sub>	
Unit cell parameters (Å and deg)	a=28.934(5) b= 6.022(2) c=14.831(3)	β=113.37(1)
Volume (Å <sup>3</sup> )	2372.5(9)	Z=8
Density <sub>calc</sub> (gcm <sup>-3</sup> )	1.67	
No. of reflections to determine cell	15	
Limits in 2θ	20.49° < 2θ < 24.14°	
Linear abs. coeff. (cm <sup>-1</sup> )	2.69	
Reflections measured max 2θ	+h, k, +l ; 50°	
Standard reflections (e.s.d.%)	7 1 -8 (1%) -2 0 8 (2%)	
No. of independent reflections	1944	
Final R <sub>1</sub> , R <sub>2</sub>	0.0488, 0.0477	

Table 4-2 (cont'd)

Final shift/error max, (ave.)	0.171 (0.042)
Secondary extinction	0.00089
Highest Peak ( $\text{\AA}^3$ )	0.38
Lowest valley ( $\text{\AA}^3$ )	-0.33
Weighting	$w = ((\sigma_F)^2 + .000507F_o^2)^{-1}$
F(000)	1216.00

Table 4-3 Crystal Data for 15b


---

Compound name	2-(4-methoxyphenyl)-1,3-dioxolan-2-ylum hexafluoroantimonate	
Compound formula	$C_{10}H_{11}O_3^+ SbF_6^-$	
Formula weight	414.88	
Crystal shape and size (mm)	rectangular prism; 0.3 x 0.5 x 0.3	
Systematic absences	h0l, l=2n+1; 0k0, k=2n+1; 00l, l=2n+1	
Space group	$P2_1/c$ (No. 14)	
Diffractometer	Syntex $P2_1$	
Unit cell parameters (Å and deg)	a=11.948(4) b=10.686(3) c=10.853(2)	$\beta=106.31(2)$
Volume (Å <sup>3</sup> )	1329.9(5)	Z=4
Density <sub>calc</sub> (gcm <sup>-3</sup> )	2.07	
No. of reflections to determine cell	15	
Limits in 2 $\theta$	20.49° < 2 $\theta$ < 27.87°	
Linear abs. coeff. (cm <sup>-1</sup> )	19.74	
Reflections measured max 2 $\theta$	h, k, +l ; 50°	
Standard reflections (e.s.d.%)	1 0 6 (2%) -2 -5 -2 (1%)	
No. of independent reflections	2261	



Table 4-3 (cont'd)

Final $R_1, R_2$	0.0551, 0.0807
Final shift/error max, (ave.)	0.006 (0.001)
Secondary extinction	0.00546
Highest Peak ( $\text{\AA}^3$ )	1.40
Lowest valley ( $\text{\AA}^3$ )	-2.39
Weighting	$w = ((\sigma_F)^2 + .00088F_o^2)^{-1}$
F(000)	796.76

Table 4-4 Crystal Data for 16b


---

Compound name	2-(1,3-pentadienyl)-1,3-dioxoanyl-2-ylum hexafluoroantimonate	
Compound formula	$C_8H_{11}O_2^+ SbF_6^-$	
Formula weight	374.86	
Crystal shape and size (mm)	plates; .32 x .3 x .06	
Systematic absences	h0l, l=2n+1; 0k0, k=2n+1; 00l, l=2n+1	
Space group	$P2_1/c$ (No. 14)	
Diffractometer	Nicolet P3	
Unit cell parameters (Å and deg)	a=10.549(2) b=10.457(3) c=11.702(2)	$\beta=105.69(.01)$
Volume (Å <sup>3</sup> )	1242.7(5)	Z=4
Density <sub>calc</sub> (gcm <sup>-3</sup> )	2.00	Density <sub>obs</sub> 1.95(15)
No. of reflections to determine cell	15	
Limits in 2 $\theta$	21.1° < 2 $\theta$ < 26°	
Linear abs. coeff. (cm <sup>-1</sup> )	23.2	
Reflections measured max 2 $\theta$	h, k, +l ; 50°	
Standard reflections (e.s.d.%)	-5 -2 0 (1%) 0 -6 1 (2%)	
No. of independent reflections	2190	
Final R <sub>1</sub> , R <sub>2</sub>	0.0337, 0.0299	

Table 4-4 (cont'd)

Final shift/error max, (ave.)	0.007 (0.002)
Secondary extinction	0.00024
Highest Peak ( $\text{\AA}^3$ )	0.60
Lowest valley ( $\text{\AA}^3$ )	-0.43
Weighting	$w = ((\sigma_F)^2 + 0.000142 F_o^2)^{-1}$
F(000)	716.77

Table 4-5 Crystal Data for 17b

Compound name	2-(4-methoxyphenyl)-4-methyl-1,3-dioxolan-2-ylum hexafluoroantimonate		
Compound formula	$C_{10}H_{13}O_3^+ SbF_6^-$		
Formula weight	428.7		
Crystal shape and size (mm)	rectangular prism; 0.33 x 0.33 x 0.3		
Systematic absences	h0l, l=2n+1; hk0, h+k=2n; h00, h=2n; 0k0, k=2n 00l, l=2n		
Space group	$P2_1cn$ (No. 33)		
Diffractometer	Syntex $P2_1$		
Unit cell parameters ( $\text{\AA}$ and deg)	a= 8.0431(4) b=12.549(3) c=14.900(2)	$\alpha=\beta=\delta=90^\circ$	
Volume ( $\text{\AA}^3$ )	1503.76(44)	Z=4	
Density <sub>calc</sub> ( $\text{gcm}^{-3}$ )	1.90	Density <sub>obs</sub>	1.83(16)
No. of reflections to determine cell	15		
Limits in $2\theta$	$22.02^\circ < 2\theta < 33.49^\circ$		
Linear abs. coeff. ( $\text{cm}^{-1}$ )	17.48		
Reflections measured max $2\theta$	h, k, +l ; 48 $^\circ$		
Standard reflections (e.s.d.%)	2 0 -8 (.3%) 3 4 6 (.3%)		
No. of independent reflections	1925		

Table 4-5 (cont'd)

Final $R_1, R_2$	0.667, 0.664
Final shift/error max, (ave.)	0.442 (0.055)
Secondary extinction	0.00312
Highest Peak ( $\text{\AA}^3$ )	91
Lowest valley ( $\text{\AA}^3$ )	-1.64
Weighting	$w = ((\sigma_F)^2 + .000371F^2)^{-1}$
F(000)	831.99

Table 4-6 Crystal Data for 18b

Compound name	2-(4-methoxyphenyl)-4,4-dimethyl-1,3-dioxolan-2-ylum hexafluoroantimonate		
Compound formula	$C_{12}H_{15}O_3^+ SbF_6^-$		
Formula weight	442.75		
Crystal shape and size (mm)	rectangular prism; 0.3 x 0.3 x 0.3		
Systematic absences	0kl, k+l=2n; h0l, h=2n; h00, h=2n; 0k0, k=2n 00l, l=2n		
Space group	$P2_1nb$ (No. 33)		
Diffractometer	Syntex P2 <sub>1</sub>		
Unit cell parameters (Å and deg)	a= 8.297(4) b=15.259(3) c=120.638(2)	$\alpha=\beta=\delta=90^\circ$	
Volume (Å <sup>3</sup> )	1599.2	Z=4	
Density <sub>calc</sub> (gcm <sup>-3</sup> )	1.837	Density <sub>obs</sub> 1.79(16)	
No. of reflections to determine cell	15		
Limits in 2 $\theta$	20.49° < 2 $\theta$ < 27.87°		
Linear abs. coeff. (cm <sup>-1</sup> )	16.44		
Reflections measured max 2 $\theta$	h, k, +l ; 50°		
Standard reflections (e.s.d.%)	2 1 7 (.3%) 3 4 6 (.3%)		
No. of independent reflections	3747		
Final R <sub>1</sub> , R <sub>2</sub>	0.0796, 0.0726		

Table 4-6 (cont'd)

Final shift/error max, (ave.)	0.498 (0.050)
Secondary extinction	0.00020
Highest Peak ( $\text{\AA}^3$ )	1.24
Lowest valley ( $\text{\AA}^3$ )	-1.19
Weighting	$w = ((\sigma_F)^2 + .00088F_o^2)^{-1}$
F(000)	863.99

Table A-1 Atomic Positional Parameters and Temperature Factors ( $\text{\AA cm}^3$ )  
for 14b

Atom	X( $\times 10^4$ )	Y( $\times 10^4$ )	Z( $\times 10^4$ )	Ueq( $\times 10^3$ )
S(1)	4099.6(2)	2003(1)	5484.6(4)	22.5(3)
O(1)	440.9(7)	5766(3)	9191(2)	44(1)
O(2)	1183.2(7)	7020(3)	556(1)	35.0(8)
O(3)	1200.6(8)	6709(4)	8950(1)	41(1)
C(1)	682.2(9)	-157(5)	9255(2)	26(1)
F(1)	1061.2(6)	1265(3)	9529(1)	41.5(8)
F(2)	418.6(6)	162(3)	8303(1)	47.4(8)
F(3)	384.8(7)	383(3)	9709(1)	49.0(9)
C(11)	3605.6(9)	9049(4)	7467(2)	20(1)
O(11)	3699.5(6)	983(3)	7857(1)	23.4(7)
C(12)	4253(1)	1236(5)	8347(2)	31(1)
C(13)	4449(1)	9070(6)	8135(2)	34(1)
O(12)	3985.9(6)	7817(3)	7578(1)	26.3(8)
C(21)	3098.8(9)	8284(4)	6918(2)	19.4(9)
C(22)	3021(1)	6166(4)	6496(2)	24(1)
C(23)	2533(1)	5469(5)	5957(2)	29(1)
C(24)	2132(1)	6859(5)	5837(2)	31(1)
C(25)	2210(1)	1059(5)	1249(2)	28(1)
C(26)	2693(1)	9666(5)	6793(2)	24(1)

Table A-2 Hydrogen Atom Positional Parameters and  
Temperature Factors ( $\text{\AA cm}^{-3}$ ) for 14b

Atom	X( $\times 10$ )	Y( $\times 10$ )	Z( $\times 10$ )	U( $\times 10$ )
H(121)	431(1)	141(5)	898(2)	34(8)
H(122)	433(1)	251(5)	806(2)	27(7)
H(131)	461(1)	824(5)	871(2)	42(8)
H(132)	463(1)	923(5)	772(2)	43(8)
H(221)	328.7(9)	528(5)	653(2)	27(7)
H(231)	247(1)	399(5)	567(2)	49(9)
H(241)	182(1)	630(5)	549(2)	34(7)
H(251)	194(1)	-10(5)	617(2)	29(7)
H(261)	275.3(9)	100(4)	707(2)	20(6)



Table A-3 Anisotropic Temperature Factors ( $\text{\AA cm}^{-3} \times 10^3$ ) for 14b

Atom	U11	U22	U33	U12	U13	U23
S(1)	26.2(3)	23.8(3)	24.3(3)	-0.8(3)	8.5(2)	-2.0(3)
O(1)	38(1)	31(1)	69(1)	-1(1)	8(1)	-10.5(9)
O(2)	42(1)	46(1)	24.3(9)	10.5(9)	8.1(8)	5(1)
O(3)	58(1)	48(1)	42(1)	2(1)	31(1)	18(1)
C(1)	22(1)	31(1)	31(1)	1(1)	9(1)	-2(1)
F(1)	37.2(9)	28.1(9)	66(1)	2.9(8)	8.1(8)	-8.0(7)
F(2)	50(1)	50(1)	38(1)	16.7(8)	-4.1(8)	7.1(9)
F(3)	57(1)	44(1)	84(1)	2(1)	48(1)	14.2(9)
C(11)	28(1)	25(1)	18(1)	3(1)	13(1)	-0.(1)
O(11)	27.8(9)	26(1)	22.3(8)	-1.4(7)	7.7(7)	-3.3(8)
C(12)	31(1)	41(2)	25(1)	1(1)	6(1)	-11(1)
C(13)	20(1)	51(2)	36(2)	-4(1)	6(1)	-7(1)
O(12)	21.6(9)	35(1)	29.9(9)	-4.6(8)	9.3(7)	0.4(8)
C(21)	25(1)	24(1)	18(1)	2(1)	10.1(10)	-0.(1)
C(22)	28(1)	27(1)	24(1)	3(1)	11(1)	2(1)
C(23)	39(2)	28(2)	27(1)	2(1)	11(1)	-7(1)
C(24)	26(1)	44(2)	27(1)	7(1)	6(1)	-9(1)
C(25)	24(1)	38(2)	29(1)	-5(1)	9(1)	-5(1)
C(26)	32(1)	25(1)	23(1)	0.(1)	11(1)	1(1)

Table A-4 Atomic Positional Parameters and Temperature Factors for 15b

Atom	X(x10 <sup>4</sup> )	Y(x10 <sup>4</sup> )	Z(x10 <sup>4</sup> )	Ueq(x10 <sup>3</sup> )
SB	1676.1(4)	9506.3(4)	2461.2(4)	27.3(3)
F(1)	962(4)	7948(4)	2399(5)	46(2)
F(2)	2367(4)	11092(4)	2502(5)	49(2)
F(3)	1347(10)	9495(8)	652(9)	31(2)
F(4)	2025(9)	9477(8)	4222(9)	31(2)
F(5)	165(11)	10167(12)	1802(13)	57(3)
F(6)	3172(10)	8892(11)	3033(12)	55(3)
F(11)	1787(12)	9321(11)	840(12)	56(3)
F(21)	1520(13)	9735(11)	4109(12)	64(3)
F(31)	3106(8)	8648(9)	2491(9)	40(2)
F(41)	323(9)	10405(8)	2353(10)	41(2)
O(11)	2443(4)	11926(5)	5531(5)	34(2)
O(12)	1035(4)	11260(5)	6282(5)	40(3)
C(11)	2129(6)	11214(6)	6339(6)	29(3)
C(12)	1406(7)	12589(7)	4741(7)	39(3)
C(13)	432(7)	12095(8)	5231(8)	45(4)
C(21)	2923(6)	10429(6)	7213(7)	27(3)
C(22)	4105(7)	10378(7)	7236(8)	34(3)
C(23)	4847(6)	9610(7)	8066(7)	34(3)
C(24)	4452(6)	8845(7)	8913(6)	30(3)
C(25)	3269(6)	8908(7)	8895(7)	32(3)
C(26)	2523(6)	9694(6)	8074(8)	33(3)
O(31)	5242(5)	8093(5)	9681(5)	42(3)
C(31)	4902(7)	7263(8)	10559(8)	43(4)

Table A-5 Hydrogen Atom Positional Parameters and Temperature Factors for 15b

Atom	X(x10 <sup>4</sup> )	Y(x10 <sup>4</sup> )	Z(x10 <sup>4</sup> )	U(x10 <sup>3</sup> )
H(121)	160(7)	1338(8)	500(8)	32(21)
H(122)	132(8)	1235(9)	392(9)	56(26)
H(131)	8(7)	1268(7)	559(7)	26(20)
H(132)	-5(7)	1158(7)	461(8)	34(20)
H(221)	440(6)	1081(6)	672(6)	12(15)
H(231)	550(7)	958(6)	797(6)	11(16)
H(251)	310(6)	851(7)	950(7)	35(19)
H(261)	167(7)	969(7)	795(8)	36(20)
H(311)	428(10)	651(10)	995(11)	103(35)
H(312)	447(6)	771(6)	1108(6)	21(16)
H(313)	544(6)	681(7)	1091(7)	21(18)

Table A-6 Anisotropic Temperature Factors (  $\times 10^4$ ) for 15b

Atom	U11	U22	U33	U12	U13	U23
SB	20.7(4)	27.2(4)	34.7(4)	-0.0(2)	1.0(2)	-3.5(2)
F(1)	50(3)	36(2)	61(3)	-7(2)	14(2)	-18(2)
F(2)	59(3)	38(3)	56(3)	-2(2)	12(2)	-22(2)
O(11)	35(3)	33(3)	37(3)	0.(2)	6(2)	-6(2)
O(12)	28(3)	49(3)	46(3)	15(3)	8(2)	7(2)
C(11)	26(3)	28(3)	35(4)	-5(3)	4(3)	-5(3)
C(12)	53(5)	26(4)	43(4)	2(3)	10(3)	4(3)
C(13)	41(4)	44(4)	51(5)	14(4)	4(4)	9(4)
C(21)	25(4)	24(3)	36(4)	1(3)	6(3)	-1(3)
C(22)	23(4)	32(4)	51(5)	-4(3)	8(3)	-5(3)
C(23)	19(3)	47(4)	39(4)	-7(3)	5(3)	-2(3)
C(24)	29(3)	35(4)	29(3)	-3(3)	6(3)	4(3)
C(25)	26(4)	32(3)	42(3)	4(3)	8.0(0)	-1(28)
C(26)	24(4)	26(3)	54(5)	-5(3)	10(3)	-3(3)
O(31)	31(3)	48(3)	49(3)	7(3)	4(2)	12(2)
C(31)	38(4)	44(5)	49(4)	11(4)	3(3)	14(4)

Table A-7 Atomic Positional Parameters and Temperature Factors for 16b

Atom	X(x10 <sup>4</sup> )	Y(x10 <sup>4</sup> )	Z(x10 <sup>4</sup> )	Ueq(x10 <sup>3</sup> )
SB	1778.2(2)	343.1(2)	2448.0(2)	30.6(1)
F(1)	1672(3)	501(2)	834(2)	63(1)
F(2)	1831(3)	221(2)	4054(2)	51(1)
F(3)	1163(2)	2020(2)	2435(2)	49(1)
F(4)	46(2)	-260(2)	2042(2)	59(1)
F(5)	2351(3)	-1349(2)	2446(2)	56(1)
F(6)	3512(2)	910(3)	2844(2)	63(1)
C(11)	-2306(4)	1355(4)	3908(3)	34(2)
O(11)	-2561(3)	2172(2)	4639(2)	40(1)
C(12)	-1310(4)	2676(4)	5392(4)	45(2)
C(13)	-284(4)	2025(4)	4904(4)	47(2)
O(12)	-1076(2)	1183(2)	3978(2)	39(1)
C(21)	-3323(4)	685(4)	3087(3)	39(2)
C(31)	-3035(3)	-128(4)	2297(3)	36(2)
C(41)	-3983(4)	-816(4)	1396(3)	40(2)
C(51)	-3615(4)	-1569(4)	634(3)	40(2)
C(61)	-4477(5)	-2335(5)	-335(4)	53(2)

Table A-8 Hydrogen Atom Positional Parameters and Temperature Factors for 16b

Atom	X(x10 )	Y(x10 )	Z(x10 )	U(x10 )
H(121)	-132.1(0)	344.3(0)	526.5(0)	37.1(0)
H(122)	-126.9(0)	234.3(0)	625.6(0)	71.6(0)
H(131)	32.2(0)	143.3(0)	540.3(0)	88.1(0)
H(132)	-17.1(0)	-242.9(0)	49.6(0)	56.0(0)
H(211)	-417.2(0)	75.4(0)	312.2(0)	56.7(0)
H(311)	-209.6(0)	-30.4(0)	229.0(0)	42.8(0)
H(411)	-480.9(0)	-72.2(0)	138.8(0)	53.4(0)
H(511)	-265.1(0)	-163.1(0)	73.2(0)	47.9(0)
H(611)	-440.5(0)	-330.7(0)	-21.6(0)	122.6(0)
H(612)	-430.0(0)	-229.7(0)	-113.1(0)	73.1(0)
H(613)	536.9(0)	214.5(0)	49.9(0)	91.5(0)

Table A-9 Anisotropic Temperature Factors ( $\times 10^3$ ) for 16b

Atom	U11	U22	U33	U12	U13	U23
SB	33.8(1)	33.9(1)	30.5(1)	-1.6(1)	11.9(1)	-3.2(1)
F(1)	99(2)	65(2)	38(1)	-1(1)	27(1)	-16(2)
F(2)	78(2)	54(1)	33(1)	4(1)	22(1)	13(1)
F(3)	57(1)	35(1)	57(1)	2(1)	6(1)	7(1)
F(4)	42(1)	68(2)	77(2)	-15(1)	19(1)	-22(1)
F(5)	81(2)	40(1)	63(2)	-7(1)	30(1)	12(1)
F(6)	33(1)	81(2)	86(2)	-22(2)	19(1)	-13(1)
C(11)	35(2)	39(2)	35(2)	13(2)	13(2)	7(2)
O(11)	43(2)	44(2)	42(2)	6(1)	17(1)	8(1)
C(12)	54(3)	42(2)	45(2)	4(2)	13(2)	-1(2)
C(13)	41(3)	52(3)	53(3)	-16(2)	12(2)	-7(2)
O(12)	29(1)	50(2)	43(1)	-6(1)	12(1)	-2(1)
C(21)	28(2)	52(3)	42(2)	9(2)	11(2)	3(2)
C(31)	30(2)	43(2)	40(2)	14(2)	10(2)	2(2)
C(41)	31(2)	52(2)	42(2)	13(2)	10(2)	-1(2)
C(51)	39(2)	47(2)	41(2)	15(2)	13(2)	1(2)
C(61)	55(3)	70(3)	41(2)	6(2)	13(2)	-6(2)

Table A-10 Atomic Positional Parameters and Temperature Factors  
( $\text{\AA cm}^{-3}$ ) for 17b

Atom	X( $\times 10^4$ )	Y( $\times 10^4$ )	Z( $\times 10^4$ )	Ueq( $\times 10^3$ )
SB(1)	-2500.0(0)	-1094.4(5)	-2045.4(4)	42.6(4)
F(1)	-1156(23)	-1117(15)	-3009(10)	46(4)
F(2)	-4032(28)	-1229(16)	-1156(17)	70(7)
F(3)	-2794(21)	388(10)	-2028(7)	49(4)
F(4)	-2070(18)	-2526(11)	-2077(8)	61(4)
F(5)	-785(19)	-924(14)	-1148(11)	46(4)
F(6)	-4275(25)	-1063(14)	-2919(11)	51(5)
F(11)	-1198(32)	-1462(20)	-1084(17)	59(6)
F(21)	-4114(26)	-571(17)	-1215(14)	58(6)
F(31)	-981(32)	-1645(21)	-2818(15)	73(6)
F(41)	-858(24)	-705(16)	-2941(11)	37(4)
F(51)	-3438(32)	258(21)	-2150(16)	73(7)
F(61)	-3562(30)	-2476(19)	-1892(15)	68(6)
C(11)	-2503(42)	-6065(7)	-3976(6)	45(5)
O(11)	-2417(31)	-5961(5)	-3115(4)	45(4)
C(12)	-2597(43)	-4823(8)	-2887(6)	59(7)
C(13)	-2510(54)	-4261(9)	-3826(6)	81(9)
C(131)	-3663(26)	-3556(11)	-4034(9)	83(11)
O(12)	-2556(28)	-5211(5)	-4438(4)	61(4)
C(21)	-2736(11)	-7085(8)	-4400(6)	25(4)
C(22)	-2442(39)	-8012(8)	-3889(6)	57(6)
C(23)	-2584(44)	-9000(7)	-4305(7)	54(6)
C(24)	-2666(32)	-9061(8)	-5229(7)	50(7)
C(25)	-2747(24)	-8135(9)	-5741(6)	47(7)
C(26)	-2646(34)	-7157(8)	-5335(6)	49(6)
O(31)	-2494(33)	-9973(6)	-5698(4)	73(5)
C(31)	-2774(35)	-10954(9)	-5168(9)	64(11)

Table A-11 Hydrogen Atom Positional Parameters and Temperature Factors  
for 17b

Atom	X( $\times 10^4$ )	Y( $\times 10^4$ )	Z( $\times 10^4$ )	U( $\times 10^3$ )
H(122)	-177.8(0)	-474.1(0)	-270.2(0)	60.0(0)
H(131)	-301.9(0)	-317.8(0)	-451.1(0)	60.0(0)
H(221)	231.6(0)	-281.6(0)	-165.0(0)	60.0(0)
H(231)	-247.3(0)	-946.0(0)	-380.4(0)	60.0(0)
H(261)	-250.3(0)	-666.8(0)	-573.1(0)	60.0(0)
H(311)	295.6(0)	-618.6(0)	-25.5(0)	60.0(0)
H(312)	-181.1(0)	-1092.9(0)	-568.2(0)	60.0(0)
H(313)	-299.4(0)	-1143.5(0)	-571.9(0)	60.0(0)

Table A-12 Anisotropic Temperature Factors ( $\text{Åcm}^{-3} \times 10^3$ ) for 17b

Atom	U11	U22	U33	U12	U13	U23
SB(1)	57.0(4)	39.5(4)	31.2(3)	-2.5(2)	3.1(8)	5.7(7)
C(11)	65(6)	39(4)	30(4)	6(4)	19(11)	21(9)
O(11)	66(5)	44(3)	24(3)	2(2)	-7(9)	-9(8)
C(12)	96(11)	38(5)	44(5)	-3(4)	-38(10)	3(12)
C(13)	166(17)	44(6)	31(4)	-4(4)	-3(16)	50(17)
C(131)	160(18)	48(7)	41(7)	2(6)	-15(9)	42(10)
O(12)	117(7)	36(3)	30(3)	3(2)	12(10)	10(10)
C(21)	0.(4)	43(4)	31(4)	5(3)	3(3)	1(3)
C(22)	93(9)	49(6)	27(4)	-1(4)	15(11)	29(14)
C(23)	86(9)	38(5)	38(4)	9(4)	-6(14)	-2(13)
C(24)	63(11)	48(5)	39(5)	-2(4)	-6(8)	-4(9)
C(25)	72(12)	45(5)	26(4)	1(3)	-8(6)	-13(7)
C(26)	75(10)	41(5)	32(4)	4(4)	-16(9)	4(10)
O(31)	141(8)	38(4)	41(3)	-2(3)	-6(13)	-10(14)
C(31)	102(22)	41(5)	50(6)	0.(4)	-23(10)	-8(10)

Table A-13 Atomic Positional Parameters and Temperature Factors ( $\text{\AA cm}^{-3}$ ) for 18b

Atom	X( $\times 10^4$ )	Y( $\times 10^4$ )	Z( $\times 10^4$ )	Ueq( $\times 10^3$ )
SB(1)	0.0(0)	2116.6(6)	1290.4(7)	32.7(5)
F(1)	1534(19)	1203(12)	1253(11)	45(5)
F(2)	158(24)	2165(7)	2770(7)	52(3)
F(3)	-1607(24)	2999(13)	1175(12)	46(6)
F(4)	1595(28)	3000(15)	1309(14)	63(8)
F(5)	-1625(20)	1282(12)	1423(11)	44(4)
F(6)	207(21)	2064(6)	-193(7)	46(3)
C(11)	-23(49)	-1031(8)	-1291(11)	28(3)
O(11)	-79(31)	-1866(6)	-1158(7)	31(2)
C(12)	148(42)	-2100(10)	-26(10)	36(4)
C(13)	249(26)	-1179(8)	530(9)	23(3)
C(131)	-1446(32)	-918(16)	1025(19)	42(7)
C(132)	1602(25)	-1023(13)	1207(16)	25(5)
O(12)	-161(20)	-579(5)	-418(6)	25(2)
C(21)	-82(42)	-606(9)	-2279(10)	33(3)
C(22)	56(43)	306(9)	-2347(10)	30(3)
C(23)	-180(32)	712(9)	-3340(11)	32(4)
C(24)	-285(25)	204(10)	-4235(12)	34(4)
C(25)	325(27)	-694(10)	-4174(12)	40(4)
C(26)	68(48)	-1112(10)	-3205(11)	39(4)
O(31)	327(18)	656(7)	-5146(8)	41(3)
C(31)	389(25)	152(12)	-6113(13)	49(5)

Table A-14 Hydrogen Atom Positional Parameters and Temperature Factors ( $\text{\AA cm}^{-3}$ ) for 18b

Atom	X( $\times 10$ )	Y( $\times 10$ )	Z( $\times 10$ )	U( $\times 10$ )
H(121)	131.7(0)	274.9(0)	498.0(0)	60.0(0)
H(122)	-99.3(0)	284.3(0)	495.7(0)	60.0(0)
H(131)	-137.6(0)	-41.3(0)	159.3(0)	60.0(0)
H(132)	-248.5(0)	-131.1(0)	85.6(0)	60.0(0)
H(133)	143.2(0)	357.2(0)	318.9(0)	60.0(0)
H(231)	-19.1(0)	128.5(0)	664.7(0)	64.5(0)
H(251)	-65.4(0)	-79.8(0)	546.3(0)	69.4(0)
H(261)	10.8(0)	329.6(0)	-208.8(0)	60.0(0)
H(311)	117.1(0)	-35.5(0)	381.9(0)	60.0(0)
H(312)	-22.2(0)	45.7(0)	314.7(0)	60.0(0)
H(313)	164.3(0)	5.0(0)	415.8(0)	60.0(0)



Table A-15 Anisotropic Temperature Factors ( $\text{\AA}^2 \times 10^3$ ) for 18b

Atom	U11	U22	U33	U12	U13	U23
SB(1)	38.8(7)	27.8(5)	31.5(5)	2.2(5)	10(1)	8(1)

### REFERENCES

1. D. Bethell and V. Gold, "Carbonium Ions An Introduction", Chapter 1  
London (1967)
2. H. Meerwein and K. van Emster, Ber, 55, 2500 (1922)
3. F.C. Whitmore, J. Am. Chem. Soc., 54, 3274 (1932)
4. "Carbonium Ions", Vol. I, G. Olah and P.v.R. Schleyer, Eds., New York  
(1968)
5. "Carbonium Ions", Vol. II, G. Olah and P.v.R. Schleyer, Eds., New  
York (1968)
6. "Carbonium Ions", Vol. III, G. Olah and P.v.R. Schleyer, Eds., New  
York (1968)
7. "Carbonium Ions", Vol. IV, G. Olah and P.v.R. Schleyer, Eds., New  
York (1968)
8. "Carbonium Ions", Vol. V, G. Olah and P.v.R. Schleyer, Eds., New York  
(1968)
9. J.D. Dunitz, "X-ray Analysis and the Structure of Organic Molecules,  
Chapter 7, London (1979)
10. E.D. Hughes, C.K. Ingold, and C.S. Patel, J. Chem. Soc., 526 (1933)
11. R.N. Young, Advances in NMR Spectroscopy, 12, 261 (1979)
12. D. Bethell and V. Gold, "Carbonium Ions An Introduction", Chapter 2  
London (1967)
13. F.H. Allen, O. Kennard, and R. Taylor, Acc. Chem. Res., 16, 146  
(1983)

14. H.B. Burgi and J.D. Dunitz, *Acc. Chem. Res.*, 16, 153 (1983)
15. F.H. Allen and A.J. Kirby, *J. Am. Chem. Soc.*, 106, 6197 (1984)
16. P.G. Jones and A.J. Kirby, *J. Am. Chem. Soc.*, 106, 6207 (1984)
17. M.R. Edwards, P.G. Jones, And A.J. Kirby. *J. Am. Chem. Soc.*, 108, 7067 (1986)
18. C.U. Pittman, S.P. McManus, and J.W. Larsen, *Chem. Rev.*, 72, 357 (1972)
19. H. Perst, "Oxonium Ions in Organic Chemistry", Chapter 2, The Hague (1971)
20. R.V.G. Sunders-Rao, J.W. Turley, and R. Pepinsky, *Acta Cryst.*, 10, 435 (1957)
21. J.E. Worsham Jr., and W.R. Busing, *Acta Cryst.*, B25, 572 (1969)
22. R.A. Kromhout and W.G. Moulton, *J. Chem. Phys.*, 23, 1673
23. J.E. Worsham, H.A. Levy, and S.W. Peterson, *Acta Cryst.*, 10, 319 (1957)
24. J.N. Brown and E.A. Meyers, *Acta Cryst.*, B26, 1178 (1970)
25. F.H. Allen, O. Kennard, D.G. Watson, L. Brammer, A.G Orpen, and R.Taylor, *J. Chem. Soc., Perkin Trans II*, S1 (1987)
26. J.H. Bryden, *Acta Cryst.*, 10, 614 (1957)
27. A. Kvik, P.-G. Jonsson, I. Olousson, *Inorg. Chem.*, 8, 2775 (1969)
28. P.-G. Jonsson, I.Oluusson, *Acta Cryst.*, B24, 559 (1968)
29. R.F. Childs, M. Mahendran, S. Zweep, G. Shaw, S. Chadda, N. Burke, B. George, R. Faggiani, C.J.L. Lock, *Pure and Applied Chemistry*, 58, No. 1, 11 (1986)

P. 95 follows

30. E.B. Fleischer, N. Suny, and S. Hawkinson, *J. Phys. Chem.*, 72 (12), 4311 (1968)
31. H. Paulsen, and R. Dammeyer, *Chem. Ber.*, 106, 2324 (1973)
32. M.R. Cairra, J.F. De Wet, *Acta Cryst.*, B37, 709 (1981)
33. R.F. Childs, R. Faggiani, C.J.L. Lock, M. Mahendran, and S. Zweep, *J. Am. Chem. Soc.*, 108, 1692 (1986)
34. S.K. Chadda, R.F. Childs, R. Faggiani, and C.J.L. Lock, *J. Am. Chem. Soc.*, 108, 1694 (1986)
35. C. Blackburn, notes, McMaster University (1983)
36. H. Meerwein, V. Hederich, and K. Wunderlich, *Arch Pharm.*, 291, 541 (1958)
37. C.U. Pittman, and S.P. McManus, *Tetrahedron Lett.*, 339 (1969)
38. G.M. Sheldrick, *SHELX Program for Crystal Structure Determination*, University of Cambridge, England (1976)
39. L.E. Sutton, *Interatomic Distances and Configuration in Molecules and Ions*, Supplement Spec. Publ. No. 18: The Chemical Society, London (1965)
40. M. Nanasawa and H. Kamogawa, *Bull. Chem. Soc. Japan*, 48, 2588 (1975)
41. A.H. Forde-Moore, *Organic Synthesis*, Vol. 30, 11 (1950)
42. C.E. Rehberg, *Organic Synthesis*, Collective Vol. 3, 146 (1955)
43. E.S. Blake, *Chem. Abstracts*, 69, 4834 (1968)
44. J.W. Larsen, *J. Am. Chem. Soc.*, 92, 5136 (1970)
45. J.M. Stewart and S.R. Hall, *The XTAL System*, University of Maryland (1983)